BANDWIDTH, PULSE WIDTH AND WAVELENGTH TUNABILITY IN PASSIVELY PULSE FIBER LASER

KHALILAH ZATILIMAN BINTI HAMDAN

INSTITUTE OF GRADUATE STUDIES
UNIVERSITY OF MALAYA
KUALA LUMPUR

2016

BANDWIDTH, PULSE WIDTH AND WAVELENGTH TUNABILITY IN PASSIVELY PULSE FIBER LASER

KHALILAH ZATILIMAN BINTI HAMDAN

DESSERTATION SUBMITTED IN FULFILMENT OF THE REQUIREMENTS FOR THE DEGREE OF MASTER OF PHILOSPOHY PHOTONICS SCIENCE

INSTITUTE OF GRADUATE STUDIES
UNIVERSITY OF MALAYA
KUALA LUMPUR

2016

UNIVERSITY OF MALAYA

ORIGINAL LITERARY WORK DECLARATION

Name of Candidate: (I.C/Passport No:)

Registration/Matric No:

Name of Degree:

Title of Project Paper/Research Report/Dissertation/Thesis ("this Work"):

Field of Study:

I do solemnly and sincerely declare that:

(1) I am the sole author/writer of this Work;
(2) This Work is original;
(3) Any use of any work in which copyright exists was done by way of fair dealing and for permitted purposes and any excerpt or extract from, or reference to or reproduction of any copyright work has been disclosed expressly and sufficiently and the title of the Work and its authorship have been acknowledged in this Work;
(4) I do not have any actual knowledge nor do I ought reasonably to know that the making of this work constitutes an infringement of any copyright work;
(5) I hereby assign all and every rights in the copyright to this Work to the University of Malaya ("UM"), who henceforth shall be owner of the copyright in this Work and that any reproduction or use in any form or by any means whatsoever is prohibited without the written consent of UM having been first had and obtained;
(6) I am fully aware that if in the course of making this Work I have infringed any copyright whether intentionally or otherwise, I may be subject to legal action or any other action as may be determined by UM.

Candidate's Signature Date:

Subscribed and solemnly declared before,

Witness's Signature Date:

Name:

Designation:

ABSTRACT

In this study, tunable bandwidth, pulse width and wavelength in passively pulse fiber lasers have been demonstrated and studied. This work consists of 4 experiments where the pulse laser is generated by passive approach using Single-wall carbon nanotube (SWCNT) as saturable absorber. The first experiment, a tunable pulse width in passively mode-locked fiber laser has been realized by varying the length of polarized maintaining fiber (PMF). Bandwidth of mode-locked spectrum is varied and indirectly tunes the pulse width from 0.52 ps to 1.65 ps. The next experiment is on tunable dual-wavelengths in passively Q-switched fiber laser. A stable dual-wavelength fiber laser have been demonstrated by using arrayed waveguide grating (AWG) and the wavelength spacing between the two wavelength is switchable from 1.6 nm to 4.0 nm. From this experiment, the repetition rate and pulse width of Q-switched laser obtained changed as the wavelength spacing is varied. Then, the third experiment is on tunable pulse width in passively Q-switched fiber laser. Bandwidth spectrum of the Q-switched laser is tuned by using an ultra-narrow tunable bandpass filter (UNTBF). As the spectral bandwidth is varied the pulse width is also tuned from 2.6 μs to 5.4 μs. The last experiment is on tunable ultra-narrow linewidth passively Q-switched fiber laser. The wavelength spectrum can be tuned from 1525 nm to 1561 nm which is about 37 nm in range by using UNTBF.

ABSTRAK

Dalam kajian ini, lebar jalur, lebar denyut dan spektrum boleh ubah dalam laser denyutan gentian pasif telah dibuktikan dan dikaji. Kerja ini terdiri daripada 4 eksperimen di mana laser denyutan dihasilkan oleh pendekatan pasif menggunakan satu lapisan tiub karbon nano sebagai penyerap boleh tepu. Eksperimen pertama ialah lebar denyut boleh ubah dalam laser gentian mod-lok secara pasif telah direalisasikan dengan mengubah panjang gentian pengekal polarisasi. Lebar jalur spektrum mod-lok adalah pelbagai dan secara tidak langsung mengubah lebar denyut dari 0.52 kepada 1.65 ps ps. Eksperimen seterusnya adalah dwi-panjang gelombang boleh ubah dalam gentian laser Q-suis pasif. Dwi-panjang gelombang yang stabil telah dicapai dengan menggunakan parutan memakai pandu gelombang (AWG) dan jarak antara kedua-dua panjang gelombang diubah daripada 1.6 nm ke 4.0 nm. Daripada eksperimen ini, kadar pengulangan dan lebar denyutan laser Q-suis yang diperolehi adalah berbeza kerana jarak gelombang yang berbeza-beza. Kemudian, eksperimen ketiga adalah lebar denyut di Q-suis laser gentian pasif boleh ubah. Jalur lebar spektrum laser Q-suis yang dicapai dengan menggunakan penapis boleh ubah laluan lulus ultra-kecil. Apabila jalur lebar spektrum diubah lebar denyut juga boleh ubah daripada 2.6 μs kepada 5.4 μs. Eksperimen terakhir adalah pada lebar garisan ultra-kecil boleh ubah di pasif Q-suis laser gentian. Panjang gelombang spektrum boleh ubah daripada 1525 nm hingga 1561 nm iaitu kira-kira 37 nm dalam rangkaian dengan menggunakan penapis boleh ubah laluan lulus ultra-kecil.

ACKNOWLEDGEMENTS

All praise to Allah. I would like to express my sincere gratitude to my supervisors, Professor Ulung Datuk Dr. Harith Bin Ahmad and Dr. Mohd Zamani Bin Zulkifli, for their guidance and encouragement that made my master degree research accomplished. This work would not be realized without their support and advice. I would like to express my gratitude to University of Malaya for awarding me Skim Biasiswazah Universiti Malaya and Kementerian Pendidikan Malaysia for sponsoring my study fee under MYBRAIN15 program. Sincere thanks are extended to all research officers, for their supports on this study and assistances throughout my journey in Photonics Research Centre, University of Malaya. Not forgotten, the appreciation also given to all lab mates for their friendship, cooperation and assistances in experimental works. Finally, I would like to extend my deepest appreciation to my parents and siblings for their prayers, supports and unconditional love that have allowed me to complete this research project successfully. I praise to Allah for sending you all into my life!

TABLE OF CONTENTS

LIST OF FIGURES

LIST OF SYMBOLS AND ABBREVIATIONS

LASER	:	Light Amplification by Spontaneous Emission Radiation
LASIK	:	laser assisted in-situ keratomileusis
SWCNT	:	Single wall carbon nanotube
EDF	:	Erbium-doped fiber
Er^{3+}	:	Erbium ions
ASE	:	Amplified spontaneous emission
WDM	:	Wavelength division multiplexer
CW	:	Continuous wave
SA	:	Saturable absorber
SESAM	:	Semiconductors Saturable Absorption Mirrors
CNT	:	Carbon nanotube
MZ	:	Mach-Zehnder
EDFL	:	Erbium-doped fiber laser
TFBG	:	Tunable fiber Bragg grating
PMF	:	Polarization maintaining fiber
AWG	:	Arrayed waveguide grating
UNTBF	:	Ultra-narrow tunable bandwidth filter
PC	:	Polarization controller
OSA	:	Optical spectrum analyzer
FWHM	:	Full-width at half maximum
TBP	:	Time-bandwidth products
RFSA	:	Radio-frequency spectrum analyser
SLM	:	Sagnac loop mirror
SLM	:	Single longitudinal mode

kHz	:	kiloHertz
nm	:	Nanometer
dB	:	Decibel
mW	:	MiliWatt
μs	:	Microsecond
ns	:	Nanosecond

CHAPTER 1: INTRODUCTION

This chapter acts as a general overview to this research report which consists of five sections. This chapter begins with background studies which thoroughly discuss the history of fiber laser, benefits of lasers and its applications. Then, the problem statement that leads to this study will be explained. The objective of this research work, work scope as well as the project work flow will be deliberated in details. At the end of this chapter, the readers will have the basic knowledge required in this research work, which will assist the reader to understand this report.

1.1 Background

Theories regarding light have been discussed since mid of 300 B.C. by the famous thinkers Euclid and Ptolemy. Nonetheless, the first experimental work carried out to understand the behavior of light was introduced by a great Muslim scholar; Abu Ali Al-Hassan Ibn Al-Haytam, or known as Al- Hazen in western countries. In his book entitled Al-Manazir (Book of Optics) published in 950, the behavior of light was explained with his experimental results and mathematical expression. Besides that, Al-Hazen's works had extensively affected the development of optics in Europe between 1260 and 1650 (Crombie, 1990; Galili & Hazan, 2001).

Then, in 1900, Max Plank proposed that from a hot object small discrete packets of energy is emitted in which propagates to the invention of laser. The principle of laser was presented by Albert Einstein in 1917 where he described the theory of stimulated emissions (Mc Cumber, 1964). Nevertheless, there are two findings in modern century that trigger the active development of photonics or modern optics:

- In 1960, Theodore Harold Maiman and co-workers successfully invented, demonstrated, and patented the world's first Light Amplification by Spontaneous Emission Radiation which is now famously known as LASER (Rawicz, 2008).

- In 1968, Kao and his co-workers did their pioneering work in the realization of fiber optics as a telecommunications medium, by demonstrating the first low-loss fiber optics (Kao, 1977).

Since then, the technology of lasers has improved and developed significantly. Previously, the first laser was flash lamp pumped and thus rather bulky and inefficient. There were also limited possibilities to control the spectral and temporal properties of the output light. Nowadays, a variety of different types of lasers are available, for instance, semiconductor laser diodes. These lasers are highly efficient due to direct electrical pumping and their small size made them very attractive for many applications. However, the spatial and temporal beam quality of diode lasers is low. One of the key attributes of a laser output is to have a specific shape, spatially, temporally and spectrally to enable a specific application, while simultaneously; the overall properties of the laser have to remain attractive concerning size, rigidness, efficiency, and price.

Lasers are extensively used in the fabrication industry, especially where high precision is needed. Cutting or welding materials like metal sheets, drilling holes or engraving with lasers have become regularly used methods for material processing. Figure 1.1 is an example of engraving on a glass block for decorative purpose. In the medical field, laser is very beneficial in a few treatments such as laser assisted in-situ keratomileusis (LASIK). Standard LASIK procedure usually uses narrow beam with pulse repetition rate, 50 kHz (Marcos, Barbero, Llorente, & Merayo-Lloves, 2001). Besides, tattoo removal treatment as shown in Figure 1.2 also employs pulse laser. On the other hand, pulse fiber laser at wavelength 1.0 μm range is synonym in telecommunication applications. For instance, pulse laser manages to provide the highest tolerance to optical transmission impairments (C. Wu & Dutta, 2000). All the applications mentioned involve the laser operating in pulse mode, but with different parameters. Thus, it will be more convenient if there is one compact laser system that is relevant in various applications.

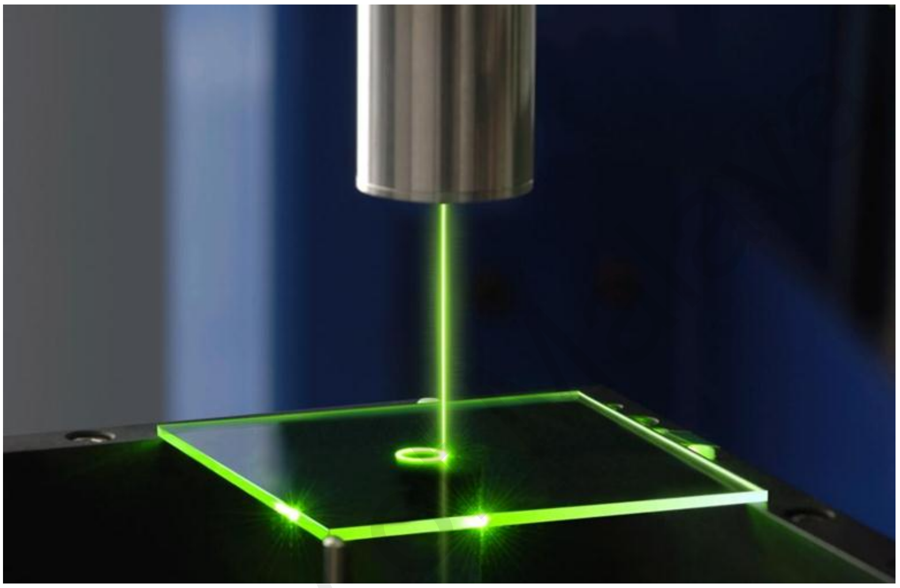

Figure 1.1: Application of laser for engraving on a glass block (NEadmin, 2015)

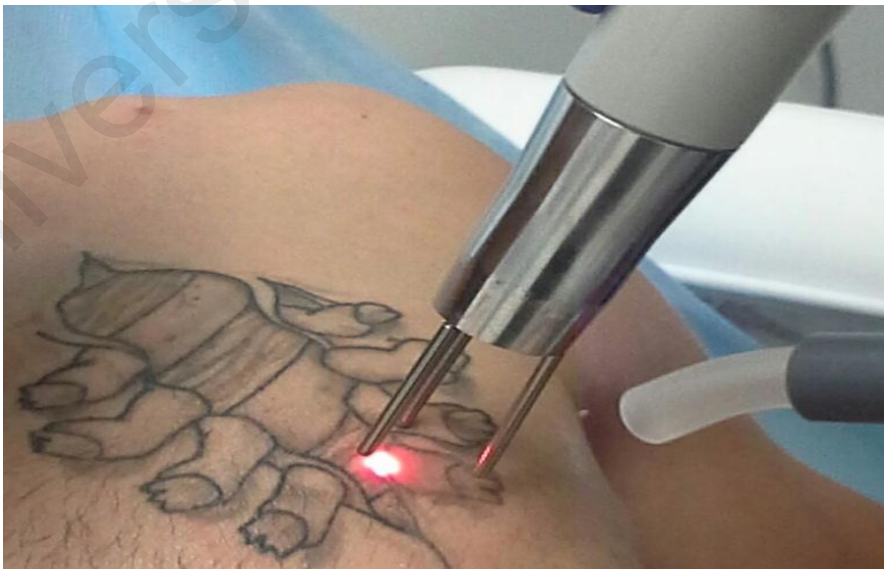

Figure 1.2: Tattoo removal treatment using pulse laser (Carol Mendelsoh, 2015)

Since compactness is always one of the desirable features in real world applications, passive approach in mode-locked and Q-switched pulse lasers generation is applied in this study. Thus, in this work, single wall carbon nanotube (SWCNT) , which acts as a saturable absorber and four techniques have been proposed and demonstrated experimentally in realizing bandwidth, pulse width and spectrum tunability in passively pulse fiber laser. The performance of the pulse fiber laser of each technique will be discussed in specifics in Chapter 4.

1.2 Problem statement

Passive pulse laser nowadays has become a favorable method in generating pulse laser because of its simple and compact configuration as well as imposes lower cost. However, flexibility in generating pulse laser using passive methods is restricted compared to active methods. In active method of generating pulse laser, the continuous light could be modulated using nonlinear device. Thus, bandwidth, pulse width, and wavelength spectrum can be tuned. On the other hand, in the passive approach, a passive intra-cavity element helps in generating pulse, but the bandwidth, pulse width, and spectrum are usually not switchable. Therefore, it is essential to find solutions to generate a pulse laser passively with the ability to switch the bandwidth, pulse width and spectrum. Thus, the versatility of passively pulse fiber laser should be increased.

1.3 Research objectives

1. To propose and demonstrate bandwidth, pulse width and spectrum tunability in passively pulse fiber laser.
2. To investigate the performance of passively pulse fiber laser with tunable bandwidth, pulse width and spectrum feature.

1.4 Scope of research

1. Study the characteristic and performance of simple laser cavity by using Erbium-doped fiber (EDF) as gain medium.
2. Study the performance behavior of passively mode-locked and passively Q-switched fiber laser by using SWCNT as saturable absorber.
3. Study the behavior and performance of passively mode-locked and passively Q-switched fiber laser with bandwidth, pulse width, and spectrum tunability.

1.5 Research flow chart

This study involves several stages and literature review is the first stage. Literature review is the fundamental step in research work where a lot of readings and discussions regarding the basic principles of fiber laser, review on previous works and understanding the behavior and function of each optical component have been done. Besides that, literature review equips one with a strong base to a research work so that each result can be explained precisely later. Once the proposed experimental configuration is decided, all optical components needed is identified, prepared and set up. Then, experimental activities were conducted to observe the performance of the proposed configurations. Data from the experiments were recorded and analysed. In research work, result discussion is the main essence and must be elaborated precisely and corresponded to the concepts in fiber laser. Next stage is report writing and preparing for publication in journals so that those findings could be shared with others. These research flows has been simplified into a diagram as illustrated in Figure 1.3.

Figure 1.3: Research flow chart

CHAPTER 2: LITERATURE REVIEW

As has been mentioned in the previous chapter, literature review is a fundamental part of this study to gain understanding on the basic concepts of fiber laser and pulse laser. Hence, this chapter will discuss comprehensively on few important concepts and theories concerning fiber laser such as erbium doped fiber covering its mechanism, modes of laser operations, which includes Q-switched pulse and mode-locked pulse laser. Additionally, this chapter also discusses on the mechanism of how does saturable absorber function and review on related previous works. By the end of this chapter the essential concept related to fiber laser is comprehended and could help to understand the discussion in the following chapters.

2.1 Erbium-doped fiber

Starting from its invention in the late 1980s, erbium-doped fiber has established itself to be a versatile gain medium with a broad range of applications, including broadband optical sources, wide-band optical amplifiers, and tunable lasers. Broadband optical sources have been applied in various areas such as optical device characterization, gyroscopes, and optical coherence tomography (Becker et al, 1999). An erbium-doped fiber is an optical fiber of which the core is doped with rare-earth element erbium ions, Er^{3+} and usually, the core is protected by three other layers; cladding, buffer, and jacket as shown in Figure 2.1.

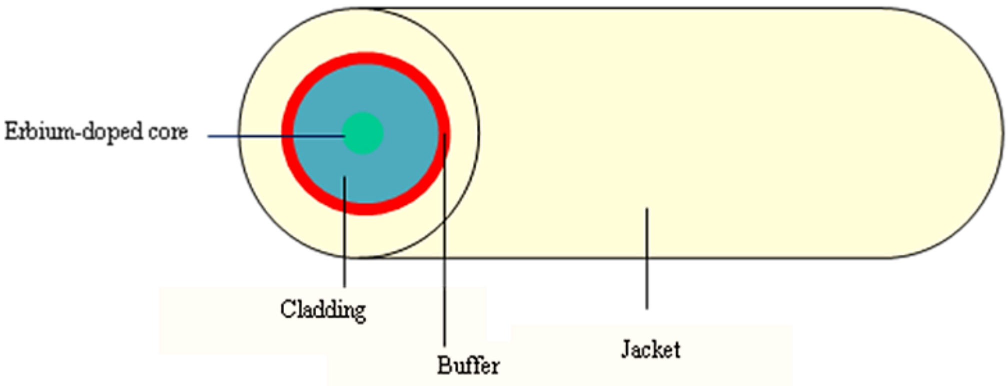

Figure 2.1: Erbium-doped fiber internal structure

The cladding confines the pump light and guides it along the fiber. Stimulated emission generated in the fiber passes through the inner core, which commonly is single mode. The inner core contains the dopant (erbium) that is stimulated to emit radiation by the pump light. The pump light behavior in erbium doped fiber is illustrated in Figure 2.2.

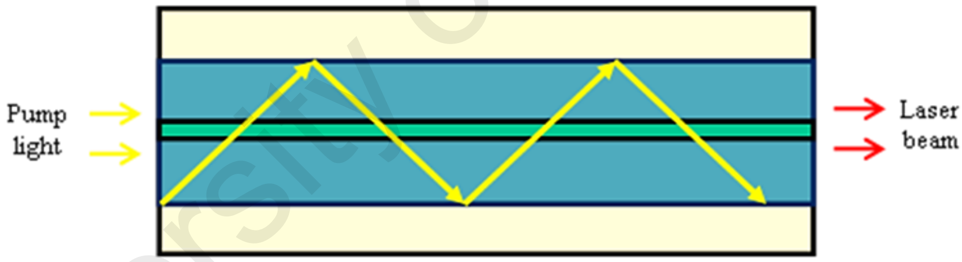

Figure 2.2: Pump light behavior in EDF

A simplified energy level diagram of Er^{3+} ion in Figure 2.3 shows the mechanism happening in erbium during the laser generation process. When a 980 nm pump laser diode beam is fed into an erbium-doped fiber, Er^{3+} ions will be excited from the ground state E1 to the higher level E3. The excited Er^{3+} ions on E3 will rapidly decay to energy level E2 through non-radiative emission. The excited ions on E2 eventually return to ground state E1 through spontaneous emission, which produces photons in the wavelength band 1520 – 1570 nm. The spontaneous emission will be amplified as it propagates through the fiber, especially when the pump laser power is increasing. As amplified spontaneous emission (ASE) covers a wide wavelength range 1520-1570 nm, we can use it as a broadband light source.

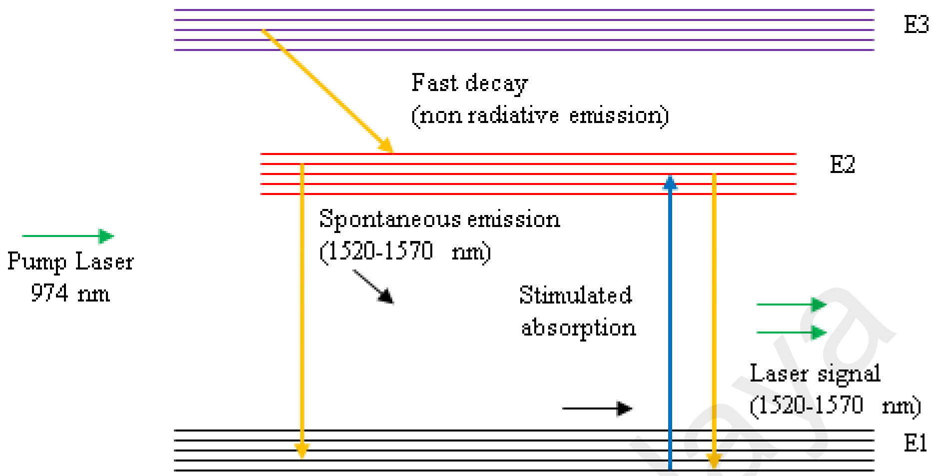

Figure 2.3: Simplified energy level diagram of Er3+ ion

Therefore, in a ring cavity, when a light signal with a wavelength between 1520 and 1570 nm, and a 980 pump laser are fed into an erbium-doped fiber simultaneously, there are three possible outcomes for the signal photon:

- Absorption: signal photon excites an erbium ion from the state E1 to a higher level E2 and become annihilated in the process.

- Stimulated emission: signal photon stimulates an erbium ion at state E2 to decay to E1, producing another identical photon. Thus, the signal is amplified.

- Signal photon can propagate unaffected through the fiber.

Spontaneous emission always occurs between level E2 and level E1. When the power of the pump laser is high enough whereby the population inversion is achieved between the energy level E2 and E1 of erbium-doped fiber, the input laser signal passing through the fiber is then amplified.

The basic operation of an erbium doped fiber amplifier is illustrated as in Figure 2.4. A high power of pump laser is combined with the input signal using a wavelength division multiplexer (WDM). Usually, a laser diode at wavelengths of 980 nm or 1480 nm is used to excite the electrons into the excited states (Dutton, 1998). The energy associated with these wavelengths corresponds to the various excited states of erbium ions. The input signal is at a wavelength within the gain spectrum of the erbium-doped fiber. Then, the combination of pump and signal is then guided to a section of erbium doped fiber. The high power pump laser excites the erbium ions to go into higher energy (lower stability) states. When the signal photons meet the energized erbium ions, the erbium ions give away their energy to the signal and return to the more stable lower energy state.

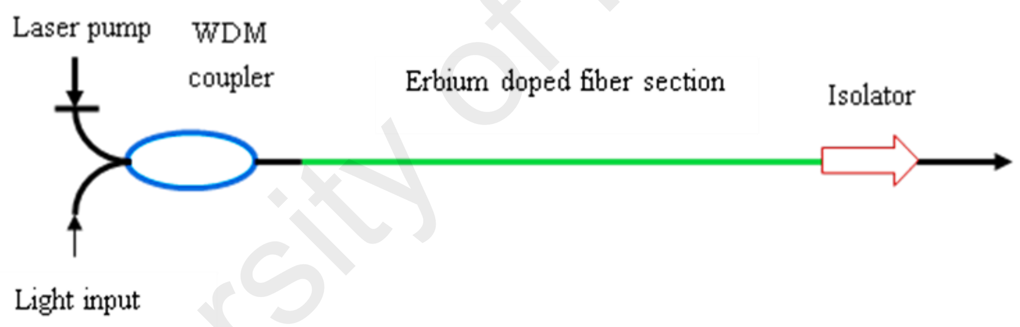

Figure 2.4: Schematic of an erbium-doped fiber amplifier

Amplification happens when erbium ions gives up their energy in the form of photons which are coherent to the signal photons i.e. in phase and in the same direction as incoming signal photons. An optical isolator is placed at the output to prevent reflections from the attached fiber and other connectors. These reflections tend to destabilize the laser. This way, the signal is amplified only in the direction in which it is traveling. Thus, all the additional power is guided in the same mode as the signal, and the system starts lasing.

The operating wavelength of the laser diode used as laser pump for erbium-doped fiber depends on the application. The 980 nm band has a higher absorption cross-section and is generally used where low noise performance is required. The 1480 nm band has a lower, but broader, absorption cross-section and is generally used for higher power amplifiers.

To generate a laser, the output from the isolator is connected back to the wavelength division multiplexer to create a laser cavity as shown in Figure 2.5. A polarization controller is employed to compensate the birefringence of the fiber. An optical isolator in the circuit ensures that light only travels in the desired direction. The laser output could be analyzed by extracting out a small portion output using an optical coupler, for example, 90:10 optical coupler.

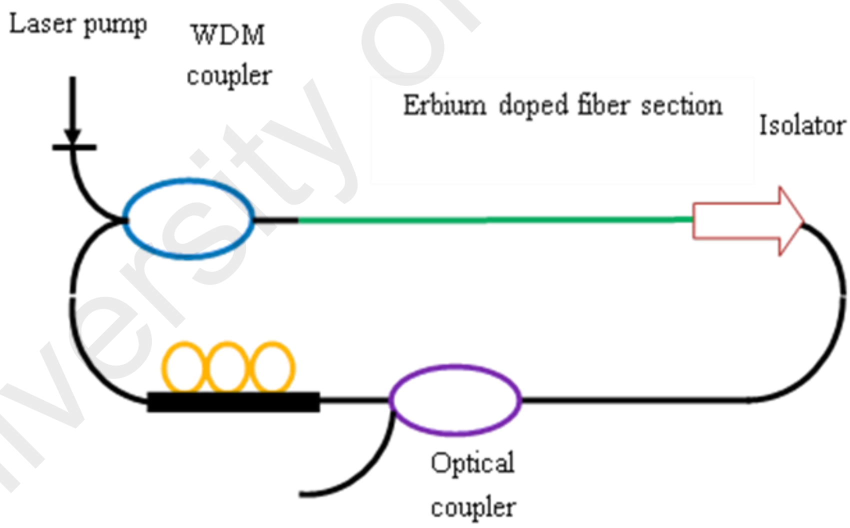

Figure 2.5: Schematic of an erbium-doped fiber laser

2.2 Modes of laser operations

Fiber laser has the ability to convert poor quality output of a pump laser diode into high-brightness coherent light. While the pumping supply is a continuous process, the output of the fiber laser can take several temporal modes, depending on the operation regime. Lasers in general can be classified, according to four principle modes of operation, which are known as continuous wave (CW), Q-switched, mode-locked, and Q-switched mode-locked. The temporal characteristics of these different modes are illustrated in Figure 2.6

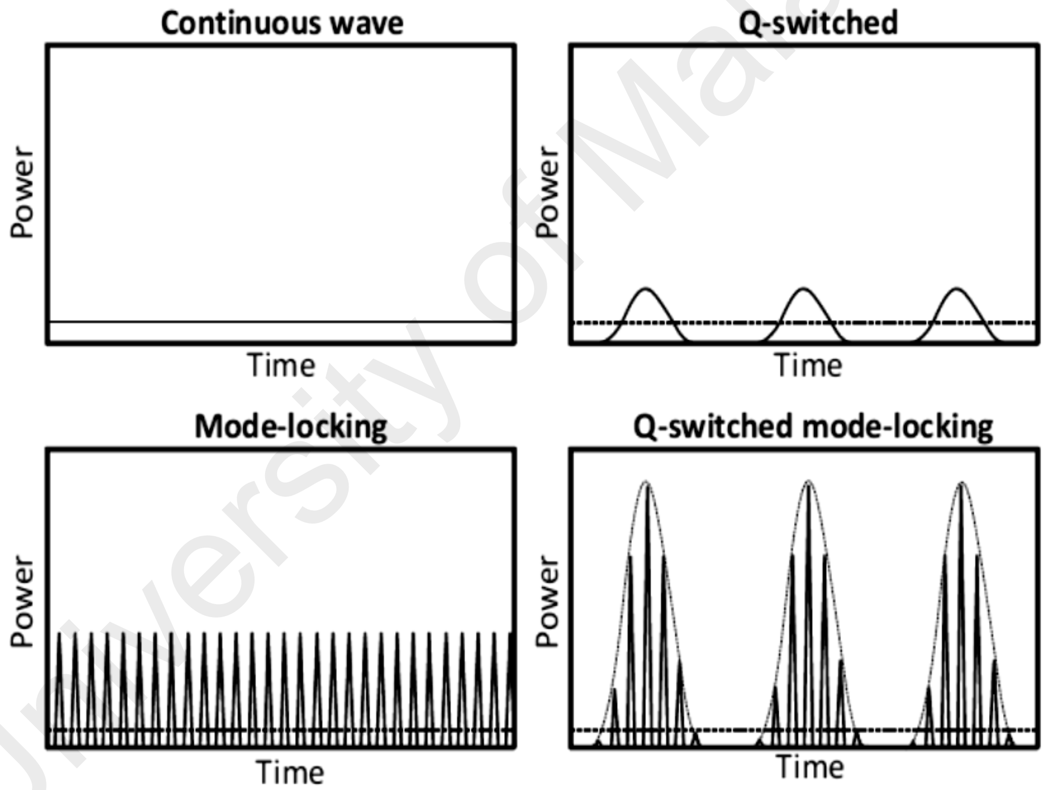

Figure 2.6: The temporal characteristics of different modes (Oehler, 2009)

As can be seen from the figure, a CW laser generates an output optical signal with constant power. In this case, instantaneous and average powers are equal. For the other cases of operation regimes, the emitted signal has a pulsed profile, characterized by parameters as pulse duration, frequency repetition rate, pulse energy, and instantaneous peak power (Villanueva Ibañez, 2012). In figure 2.6, the average power for the pulsed regimes is plotted, being equal for comparison in all four regimes. Usually, lasers in CW operation has higher average output power than pulse mode irrespective of their cavity design due to steady and continuous beam power (Saraceno et al, 2013). In CW operation, lasers can run with a single longitudinal mode of the optical resonator, providing a narrow linewidth emission with good coherence, which is interesting for spectroscopy and interferometry. In other cases of CW operation, the laser can emit a signal with a broad bandwidth, suitable for fiber-optic gyroscope (Bergh et al, 1982).

In a Q-switched laser, the lasers deliver pulses with durations of nanoseconds, and pulse energies of miliJoules. For fiber lasers, the use of multimode fibers can supply pulse energies above miliJoule level (Richardson et al, 1999). Typical applications of Q-switched lasers are material processing especially in material cutting, drilling, and laser marking. Besides, Q-switched laser is very useful in pumping nonlinear frequency conversion devices, range finding, and remote sensing.

Meanwhile, mode-locked single-mode fiber lasers can deliver pulses with a short duration of 100 fs and energy of 3 nJ (Nelson et al, 1996), only about one order of magnitude lower than the energy outputs of bulk femtosecond lasers (et al, 1994). Furthermore, single mode fiber lasers can have very low timing jitter compared with bulk lasers (Haberl et al., 1991) and also the capability for a high degree of integration. Thus, in applications sensitive to timing jitter and laser sizes with reduced power requirements, fiber lasers hold an advantage over bulk femtosecond lasers.

Next, the Q-switched mode-locking is an operation regime of mode-locked lasers with strong fluctuations of the pulse energy. During the Q-switched mode-locking operation regime of a passively mode-locked laser, the intra-cavity pulse energy undergoes large oscillations, related to a dynamic. The pulse energy may even become extremely small for a number of subsequent pulses, before the next train of pulses is generated. The regime of Q-switched mode locking, in some cases, is fairly stable which leads to trains of pulses with reproducible properties. In other words, it is very unstable due to presence of strong fluctuations of parameters such as maximum pulse energy, pulse duration, and optical phase (Schibli et al, 2000). Principally, in the latter case, the term Q-switching instabilities is often used. Normally, the stability is good in cases where the pulses do not become too weak between traces of pulse. Otherwise, the pulses in each bunch are basically created from noise particularly from spontaneous emission, and the pulse parameters cannot reach a stable state. This means that generally in those situations where Q-switched mode locking leads to large maximum pulse energies, the operation is typically noisy. Therefore, Q-switched mode locking is not widely used in applications and is typically considered an unwanted phenomenon (Hönninger et al, 1999).

2.2.1 Q-switched pulse

In Q-switched pulse generation, the quality factor of the resonant cavity changes with time. At first, the gain medium is pumped, while the extraction of energy as laser light is prevented by keeping the resonator losses high (quality factor, Q-factor is low), the laser is unable to oscillate, and the active medium stores energy from the pump source in the form of population inversion. Then, when the Q-factor is deliberately enhanced, the gain is substantially higher than the resonator losses and all the stored energy is released in the form of a powerful optical pulse. The intra-cavity power rises exponentially, until the gain is saturated and the power decays again (Paschotta, 2008). This process is illustrated in Figure 2.7.

Figure 2.7: Illustration of Q-switched process

The upper lifetime of the active medium should be long enough to reach high energy storage rather than losing the energy as fluorescence. Depending on the way of modulating the Q-factor, Q-switching can be achieved via passive or active approaches. Active approach usually uses acoustic or electro-optic modulators integrated within the laser cavity to obtain the pulse output which contribute to the complexity of the laser system. On the other hand, passive approach uses saturable absorbers (SAs) such as Semiconductors Saturable Absorption Mirrors (SESAMs), graphene thin films, and carbon nanotube (CNT) thin films (Hecht, 1992; Maiman, 1960; Snitzer, 1961). The benefits of using SAs in generating Q-switching laser are simplicity, compactness, ease of operation and low cost which makes this approach preferable (Harun et al, 2012).

2.2.2 Mode-locked pulse

In the case of mode-locked lasers, the mechanism of pulse shaping is different from Q-switching lasers. In a laser cavity, multiple longitudinal modes can oscillate and the output of this multi-line source, when all modes oscillate independently from the others, is a composition of random phase related optical components, giving an averaged constant power output. If we are able to set a common phase reference to all longitudinal modes, the coherent sum of all longitudinal modes leads to an optical train of pulses, with a period equal to the cavity roundtrip time (Paschotta, 2008). In other words, "Mode-locking" means to lock together the phases of sinusoidal signals so they can be coupled, that is, they can interfere constructively and generate a pulsed output. Wherever else the modes are not locked, the interference will be destructive and the modes will cancel themselves out. The more modes are in the cavity the stronger this effect will be, and the pulses will be more defined (Siegman, 1986).

Figure 2.8 shows three sine waves with slightly different frequencies and initial amplitudes. At t=0 the three modes are completely in phase, at this time the resultant field amplitude will be three times the amplitude of any single mode, hence the peak intensity is nine times the intensity of any single sideband.

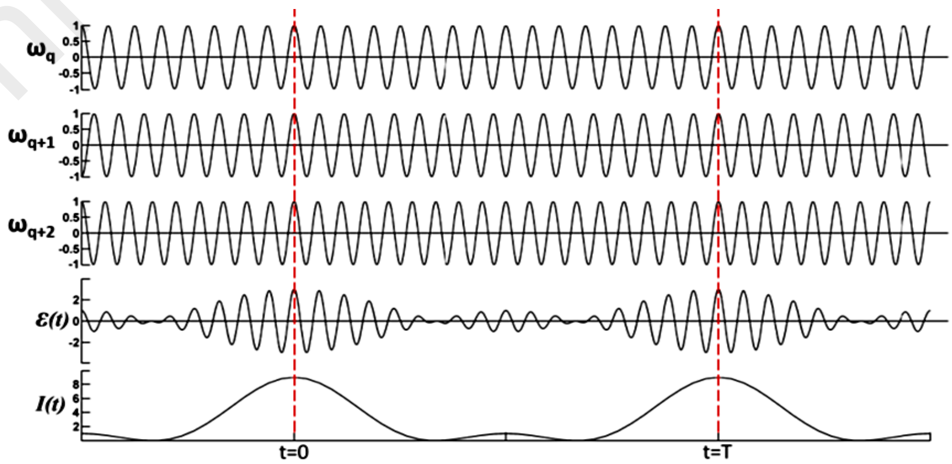

Figure 2.8: Superposition of three equally spaced frequency components which are all exactly in phase at t=0 (Siegman, 1986)

The pulse shape can be represented by a bell-shaped function, such as a Gaussian function. Since half-maximum quantities are experimentally easier to measure, the relationship between the duration and spectral bandwidth of the laser pulse can be written as:

$$\Delta v \Delta t \geq K \tag{2.1}$$

where $\Delta\nu$ is the frequency bandwidth measured at full-width at half-maximum (FWHM) with $\omega = 2\pi\nu$ and Δt is the FWHM in time of the pulse and K is a number which depends only on the pulse shape. Thus in order to generate a laser pulse within femtosecond time domain one needs to use a broad spectral bandwidth (Boll et al, 2013).

2.3 Saturable absorber (SA)

Saturable absorber is an optical component which helps in generating pulse by passive approach. Normally, saturable absorber has a certain optical loss, which is reduced at high optical intensities. This happens in a medium with absorbing dopant ions, when a strong optical intensity leads to the depletion of the ground state of these ions. Similar effects can occur in semiconductors, where excitation of electrons from the valence band into the conduction band reduces the absorption of photon energies just above the bandgap energy (Kashiwagi & Yamashita, 2010).

Saturable absorber is capable to create either passive mode-locking or Q-switching pulse. However, saturable absorbers are also useful for purposes of nonlinear filtering outside laser resonators, such as for cleaning up pulse shapes and in optical signal processing (Steinmeyer et al, 1999). There are many types of saturable absorber for passive approach pulse generation. However, semiconductor saturable absorber mirrors (SESAMs) and carbon based saturable absorbers are the most frequently used. Besides that, there are also artificial saturable absorbers where a device is used for decreasing optical losses for higher intensities, but not actually exploiting saturable absorption. These types of device can be based on Kerr lensing (Brabec et al, 1992), non-linear mirror device (Stankov, 1988) and non-liner fiber loop mirror (Fermann et al, 1990).

When a saturable absorber is placed in a laser cavity, amplified spontaneous emission (ASE) noise of a gain medium will be shaped to be a pulse train. In every round trip, light passes the saturable absorber as high intensity noise with low loss and low intensity noise with high loss, resulting in high intensity contrast as illustrated in Figure 2.9. Thus, the light signal starts to oscillate in a pulsed state. The simplified phenomenon occurred in the laser cavity is shown in Figure 2.10.

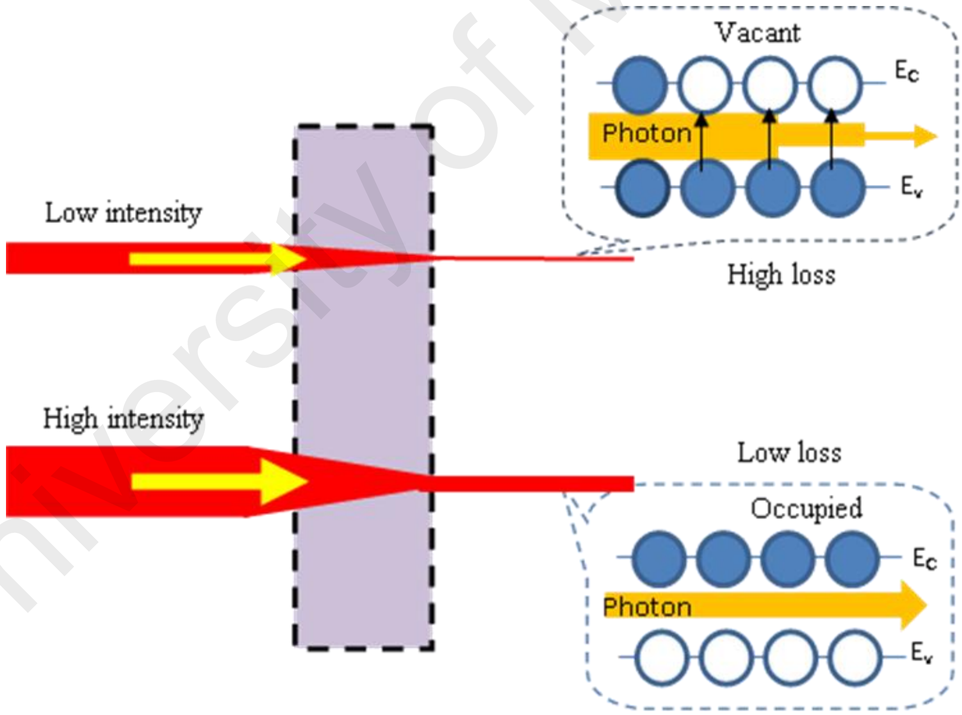

Figure 2.9: Illustration of saturable absorption (Kashiwagi & Yamashita, 2010)

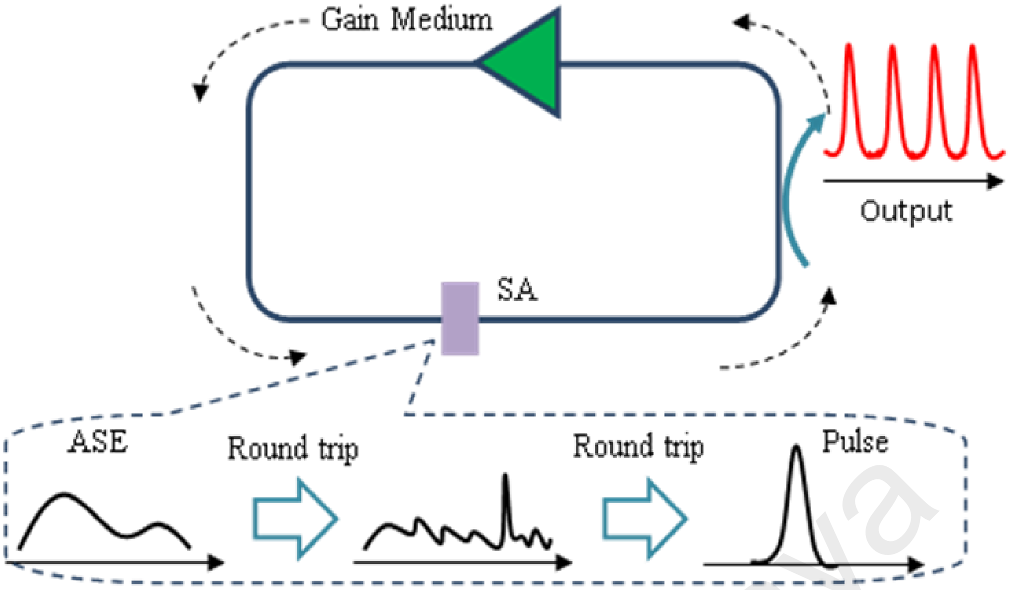

Figure 2.10: Mechanism of SA in laser cavity (Kashiwagi & Yamashita, 2010)

They are few properties of saturable absorbers that could influence in pulse generation. The first characteristics of saturable absorber is modulation depth. Modulation depth is the maximum change in absorption or reflectivity which can be induced by incident light with a given wavelength (Huang et al, 2007). This is an important design parameter in passively mode-locked lasers. A large modulation depth leads to strong pulse shaping by the saturable absorber, which can lead to a short pulse duration and reliable self-starting, but also to Q-switching instabilities.

Next, the recovery time which is the decay time of the excitation after an exciting pulse. In Q-switched pulse generation, the recovery time should not be too long. Ideally it would also not be shorter than the pulse duration. However, is often not essential, particularly when the saturation fluence is far below the pulse fluence. On the other hand, depending on the mode locking appliance used, the recovery time may or may not be essential for achieving short pulses. For absorbers with a bitemporal response, the slow components may be useful for reliable self-starting characteristics Thus, for passive mode locking, but not too short for passive Q-switching (Paschotta, 2016).

Besides, the damage threshold in terms of intensity or fluence could constitutes an upper limit for the operation parameters (Cowan, 2006). The damage threshold in terms of intensity and fluence must be sufficiently high for Q-switched. Meanwhile in mode-locked pulse generation, the saturation conditions under normal operating conditions are usually of no concern to avoid saturable absorber damage. However, it can be essential to suppress Q-switching instabilities. Surprisingly, there are cases where absorber damage can be avoided by stronger focusing of the intracavity beam on the absorber, because this helps to suppress Q-switching instabilities. In some cases, particularly for high powers and for high pulse repetition rates, heating may be a concern (Paschotta, 2016).

2.4 Previous work

Previously, there were many studies on tunable pulse lasers that have been conducted using different methods and approaches. Many variables of the pulse lasers can be studied and manipulated, for instance, the centre wavelength of laser, the pulse width, spectral bandwidth, and repetition rate. Differences in terms of output performance of pulse laser could be achieved by tuning each of the variables mentioned. In 2009, Yamashita et al., reported a study on tunable wavelength of a mode-locked fiber laser. In this work a semiconductor optical amplifier (SOA) was used as the gain medium and the mode-locked operation was achieved by an active approach where the current injection into SOA was modulated. Based on the dispersion tuning of dispersion compensation fiber (DCF), the wavelength of mode-locked laser was switchable by increasing or decreasing the frequency pulse. Besides that, they also used several different lengths of DCF in their work and the range of wavelength tuning achieved was found to be varied (Yamashita & Asano, 2006).

In 2010, Feng and co-workers demonstrated a tunable pulse width of actively Q-switched erbium fiber laser by changing the cavity Q factor using an abrupt-tapered Mach-Zehnder (MZ) filter and a tunable Fabry-Perot (FP) filter. The FP filter is modulated to quickly turn on/off the laser contingent upon the overlap condition between FP and the MZ filters. The laser pulse width can be tuned over 78 ns ~ 23 ms. In this work, the experimental set up was quite complex (Feng et al, 2010). Next, in 2012, a graphene-based Q-switched erbium-doped fiber laser (EDFL) with a tunable fiber Bragg grating (TFBG) acting as a wavelength tuning mechanism was demonstrated by Ahmad and co-researchers. A TFBG was used as a wavelength tuning mechanism with a tuning range of 10 nm, covering the wavelength range from 1547.66 nm to 1557.66 nm and the repetition rate and pulse width at different wavelength were varied (H Ahmad et al, 2013).

Based on these previous works, by tuning variables in pulse laser it will result difference output performance and those outcomes was interesting as it could improve the existing laser performances and might be suitable to be applied in many industrial applications. Therefore, pulsed laser tunability is actually a broad research field as various techniques and variables can be manipulated to gain different output performances.

CHAPTER 3: RESEARCH METHODOLOGY

This chapter is the third chapter of this report where the experimental techniques and configurations that are proposed in this research work will be explained in details. At the beginning of this chapter, the sandwiching technique of saturable absorber as the passive approach in generating pulse laser will be elaborated then, it will be continued with the proposed set up for techniques to deliver bandwidth, pulse width and wavelength tunability. The first proposed configuration is for the tuning of the mode-locked pulse width by varying the length of polarization maintaining fiber (PMF) in a Sagnac loop mirror. Then, the second proposed techniques is to vary the wavelength spacing of dual-wavelength Q-switched pulse by using arrayed waveguide gratting (AWG). The next proposed experimental set up is for the tuning of wavelength bandwidth of a Q-switched pulse laser by using ultra-narrow tunable bandwidth filter (UNTBF) and the last proposed configurations is to obtain a switchable wavelength of an ultra-narrow Q-switched pulse laser using the UNTBF.

3.1 Single wall carbon nanotube (SWCNT) saturable absorber (SA) sandwiching technique

A small cut of SWCNT thin film of saturable absorber is placed on the fiber ferrule of a fiber patch cord and index matching gel is used on the fiber ferrule as adhesive between SWCNT-SA and the fiber ferrule. Then, another patch cord is coupled to the fiber ferrule using fiber connectors. Thus, the SWCNT is sandwiched between two fiber ferrules as shown in Figure 3.1.

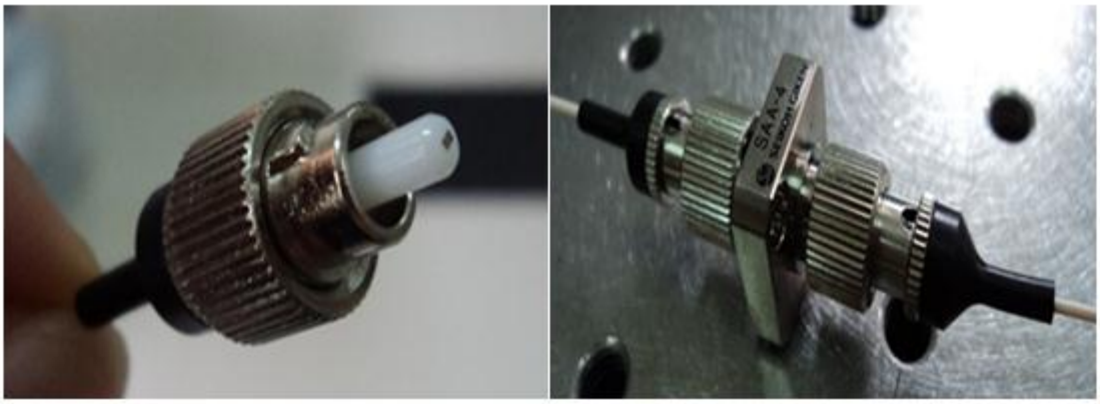

Figure 3.1: SWCNT-SA sandwiching technique

In passive Q-switching, the nonlinear response of the saturable absorber can be used to modulate the loss and the Q-factor of a laser cavity to generate a regular train of Q-switched pulses (Woodward et al, 2014). As the gain medium is pumped, it builds up stored energy and emits photons. After many round-trips, the photon flux begins to see gain, fixed loss, and saturable loss in the absorber. If the gain medium saturates before the saturable absorber, the photon flux may build, but the laser will not emit a short and intense pulse. On the contrary, if the photon flux builds up to a level that saturates the absorber before the gain medium saturates, the laser resonator will see a rapid reduction in the intracavity loss and the laser Q-switches and therefore, will emit a short and intense pulse of light (Ismail, 2016; Welford, 2003). Meanwhile in passive mode-locking, because of saturable absorber a short pulses circulating in the laser cavity, each time the pulse hits the saturable absorber, it saturates the absorption, thus temporarily reducing the losses. The shorter the pulse becomes, the faster the loss modulation, provided that the absorber has a sufficiently short recovery time. The pulse duration can be even well below the recovery time of the absorber (Paschotta, 2016).

3.2 Experimental set up of tunable pulse width in passively mode-locked fiber laser via Sagnac loop mirror

The experimental setup of the controllable pulse width using different lengths of PMF in Sagnac loop mode-locked fiber laser is shown in Figure 3.2. A 980 nm laser diode is used as a pump source which is connected to the 980 nm port of a wavelength division multiplexer (WDM). The common port of WDM is connected to a ~3m MetroGain-12-type erbium-doped fiber (EDF) which acts as the gain medium. The other end of the EDF is connected to port 2 of the 2x2 3 dB coupler. As shown in Figure 3.2, port 1 of the 2x2 3 dB coupler is connected to one end of the PMF with a length of 0.5 m, while the other end of the PMF is connected to port 4 of the 2x2 3 dB coupler, thereby forming the Sagnac loop mirror. A polarization controller (PC) is placed in the Sagnac loop order to control the polarization state of the light entering the PMF. Port 3 of the 2x2 3 dB coupler is connected to a 90:10 fused coupler with the 90% port connecting back to the 1550 nm port of WDM, thus completing the ring fiber laser configuration.

In between the 90% port of the coupler and 1550 nm port of the WDM, a single wall carbon nanotube (SWCNT) thin film is placed as saturable absorber (SA) for generating mode-locked pulses, which is constructed by sandwiching the film between two fiber ferrules. An isolator is inserted after the SWCNT SA to ensure unidirectional laser propagation. The output of the mode-locked laser is extracted via the 10% port of the 90:10 coupler and connected to an optical spectrum analyzer (OSA Yokogawa AQ63703) with resolution of 0.02 nm for spectral analysis. A LeCroy 352A oscilloscope together with an Agilent 83440C lightwave detector is used to measure the properties of the mode-locked pulse train. The radio frequency spectrum of the mode-locked pulses is also observed by using an Anritsu MS2683A radio frequency spectrum analyzer (RFSA). Besides, the autocorrelation trace of the mode-locked output is measured using the autocorrelator. This experiment is then repeated by changing the length of PMF to 1.0 m and 2.0 m respectively.

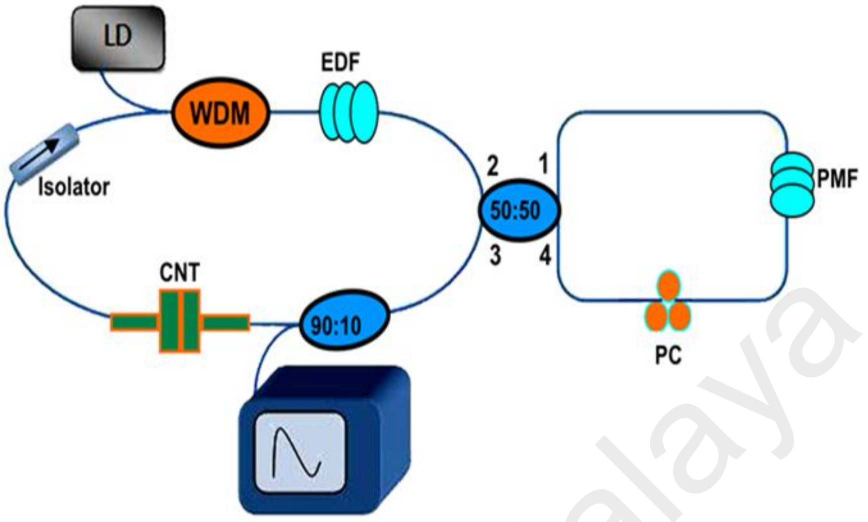

Figure 3.2 Experimental set up of tunable pulse width in passively mode-locked fiber laser via Sagnac loop mirror

3.3 Experimental set up of switchable dual-wavelength in passively Q-switched fiber laser by using arrayed waveguide grating (AWG)

The experimental setup of the proposed switchable dual-wavelength CNT-based Q-switched fiber laser using AWG is shown in Figure 3.3. A 3 meter long MetroGain-12-type erbium-doped fiber (EDF) is used as the gain medium of the fiber laser, with an erbium absorption coefficient of between 11 to 13 dBm^{-1} at 980 nm and about 18 dBm^{-1} at 1550 nm. The erbium ion concentration of the EDF is 960 ppm. The EDF is pumped by a 980 nm laser diode with a maximum output power of 141.3 mW through the 980 nm port of a 980/1550 nm wavelength-division multiplexer (WDM), with the common output of the WDM connected to the EDF. The other end of the EDF is connected to an input of an optical isolator to enforce unidirectional propagation of light within the ring cavity. The output of the optical isolator is then connected to the input port of an AWG, a silica-based waveguide that acts as a wavelength selective element. This AWG plays the role of splitting the incident beam into different multiple channels, or in other words, to diffract it into multiple wavelengths. Two output channels from the AWG are selected to allow for the generation of dual-wavelengths fiber laser whereby each of the output is connected to the 50% port of a 2x1 3 dB optical coupler. The channels of the AWG can be switched, such that different channels correspond to different lasing wavelengths.

The 100% port of the 3 dB optical coupler is then connected to the 100% port of a 90:10 optical coupler, which is used to extract a portion (10%) of the signal oscillating in the cavity for analysis. The remaining signal emitted from the 90% port of the coupler will then encounter the CNT-based SA, which is responsible for generating the Q-switched pulses. The output of the SA is connected to the 1550-nm port of the WDM, thus forming the ring laser cavity. The portion of the signal extracted by the 10% port of the coupler is connected to an optical spectrum analyzer (OSA Yokogawa AQ63703) with a resolution of 0.02 nm for spectral analysis. A LeCroy 352A oscilloscope together with an Agilent 83440C Lightwave detector is used to measure the properties of the Q-switched pulse train. This experiment is repeated by switching one of the output channels of the AWG to any one of the other 3 channels of the AWG in order to obtain different wavelength spacing of the dual-wavelength laser output.

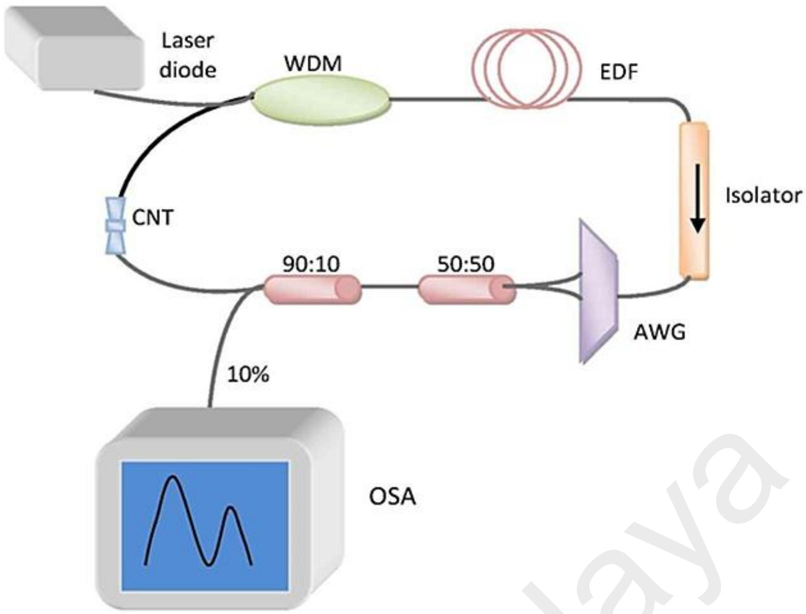

Figure 3.3: Experimental set up of switchable dual-wavelength in passively Q-switched fiber laser by using arrayed waveguide grating (AWG)

3.4 Experimental set up of tunable pulse width in passively Q-switched fiber laser by using ultra-narrow tunable bandpass filter (UNTBF

The experimental set up for pulse width tuning in passively Q-switched erbium-doped fiber laser is shown in Figure 3.4. A ~3 meter long MetroGain-12-type erbium-doped fiber (EDF) is used as the gain medium of the fiber laser. The erbium absorption coefficient of this EDF is approximately 12 dBm^{-1} at 980 nm and about 18 dBm^{-1} at 1550 nm. The erbium ion concentration of the EDF is 960 ppm. The EDF is pumped by a 980 nm laser diode with a maximum output power of 107.2 mW via a 980 nm port of a 980/1550 nm wavelength-division multiplexer (WDM), with the common output of the WDM connected to the EDF. The other end of the EDF is connected to an input of an optical isolator to enforce unidirectional propagation of light within the ring cavity. Then, the output signal from the optical isolator is coupled to the CNT-based SA, which is responsible for generating the Q-switched pulses. The other end of the patch cord that sandwiches the CNT-based SA is coupled with the input port of the XTM-50 Yenista ultra narrow tunable bandpass filter (UNTBF).

The filter consists of bulk optics in combination with diffraction gratings, which leads to high selectivity, low insertion loss, and low dispersion features. Then, the output signal from the filter passing through to the 100% port of a 90:10 optical coupler. The light from the 90% port of the coupler is coupled to the 1550-nm port of the WDM, thus forming the ring laser cavity. The portion of the signal extracted by the 10% port of the coupler is connected to an optical spectrum analyzer (OSA Yokogawa AQ63703) with a resolution of 0.02 nm for spectral analysis. A LeCroy 352A oscilloscope together with a Thorlabs D400 FC InGas photo detector is used to measure the properties of the Q-switched pulse train. This experiment is repeated by adjusting the controller of the tunable bandpass filter to obtained different 3 dB bandwidth of the Q-switched laser spectrum.

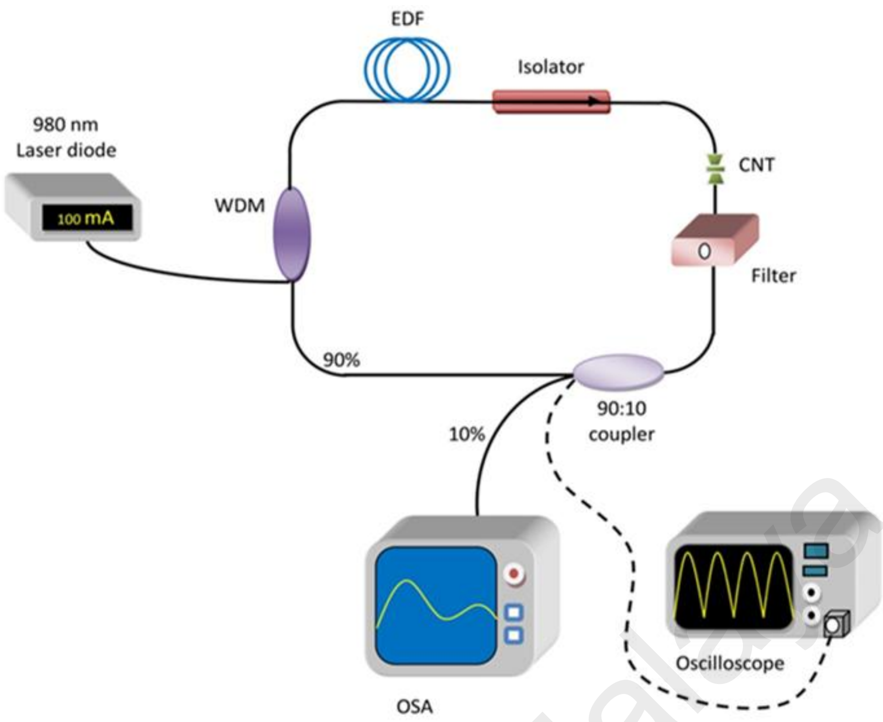

Figure 3.4: Experimental set up of tunable pulse width in passively Q-switched fiber laser by using ultra-narrow tunable bandpass filter (UNTBF

3.5 Experimental set up of tunable ultra-narrow linewidth in passively Q-switched fiber laser by using ultra-narrow tunable bandpass filter (UNTBF)

The experimental set up for tunable narrow linewidth in passively Q-switched erbium-doped fiber laser is shown in Figure 3.5. A ~3.0m-long MetroGain-12-type erbium-doped fiber (EDF) is used as the gain medium of the fiber laser. The erbium absorption coefficient of this EDF is approximately 12 dBm^{-1} at 980 nm and about 18 dBm^{-1} at 1550 nm. The erbium ion concentration of the EDF is 960 ppm. The EDF is pumped by a 980 nm laser diode with a maximum output power of 83.2 mW via a 980 nm port of a 980/1550 nm wavelength-division multiplexer (WDM), with the common output of the WDM connected to the EDF. The other end of the EDF is connected to an input of an optical isolator to enforce unidirectional propagation of light within the ring cavity.

Then, the output signal from the optical isolator is coupled to the SWCNT-based SA, which is responsible for generating the Q-switched pulses. The other end of patch cord that sandwiches the SWCNT-based SA is coupled to the input port of the XTM-50 Yenista ultra narrow tunable bandpass filter (UNTBF). The filter consists of bulk optics in combination with diffraction gratings, which leads to high selectivity and low dispersion features. Then, the output signal from the filter passes through to the 100% port of a 90:10 optical coupler. The light from the 90% port of the coupler is coupled to the 1550-nm port of the WDM, thus forming the ring laser cavity. The portion of the signal extracted by the 10% port of the coupler is connected to an optical spectrum analyzer (OSA Yokogawa AQ63703) with a resolution of 0.02 nm for spectral analysis. A LeCroy 352A oscilloscope attached with a Thorlabs D400 FC InGas photo detector is used to measure the properties of the Q-switched pulse train. This experiment is repeated by adjusting the controller of the ultra-narrow tunable bandpass filter to tune the wavelength.

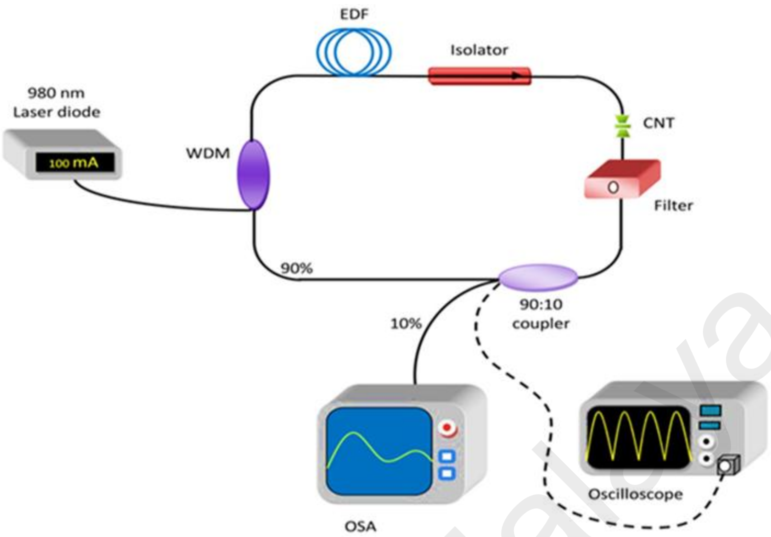

Figure 3.5: Experimental set up for tunable ultra-narrow linewidth in passively Q-switched fiber laser

Further verification of the SLM operation of this system is achieved by using the heterodyned technique using local oscillator. The setup of this technique is as shown in Figure 3.6. The setup is consists of single longitudinal mode fiber laser, 3 dB coupler, 500 m SMF, PC and acousto-optic modulator (AOM).

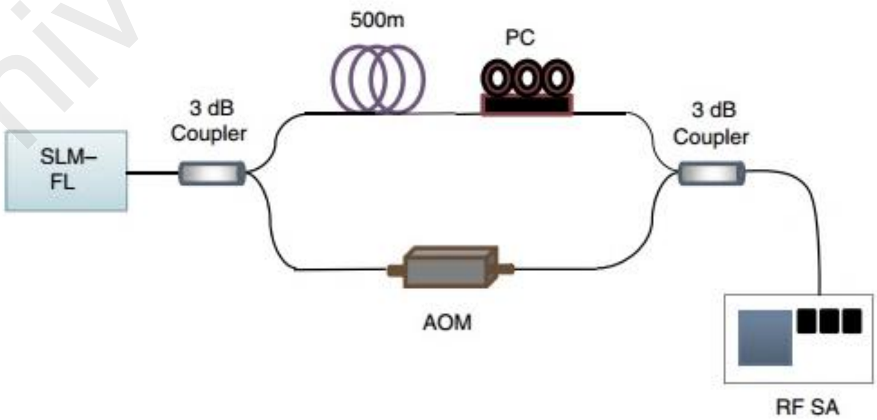

Figure 3.6: Set-up of heterodyned technique using local oscillator for SLM verification.

CHAPTER 4: RESULT AND DISCUSSION

In this chapter, the results of the proposed configurations which have been discussed thoroughly in the previous chapter will be explained comprehensively. There are four sections in this chapter. Each section will elaborate the performance of each proposed technique in tuning bandwidth, pulse width and wavelength spectrum of the pulse laser in terms of wavelength spectrum, average output power, repetition rate, pulse width and radio-frequency. Thus, in this chapter the advantages of the proposed techniques in terms of the performance of the pulse laser will be discussed.

4.1 Tunable pulse width in passively mode-locked fiber laser via Sagnac loop mirror

The typical experimental set up for fiber-based Sagnac loop mirror is shown in Figure 4.1. As shown in the figure, the light source is initially split into two beams by a 2x2 3 dB coupler (Moon et al., 2007; Sun et al., 2008). Subsequently, the light beams travel in opposite directions; one in a clockwise direction and the other in a counter-clockwise direction around the PMF. Both the clockwise and counter-clockwise beams will propagate at a different velocity in the PMF, which is a result of difference polarizations between the two beams (Frazão et al, 2007).

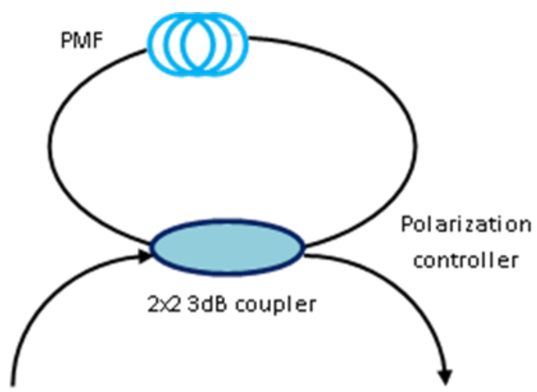

Figure 4.1: Typical fiber-based Sagnac loop mirror

PMF is used in Sagnac loop because it can maintain the polarization planes of light waves launched into the fiber with minimum or no cross-coupling optical power between the polarization modes due to the strong high-birefringence (Hi-Bi) characteristic. Birefringence of PMF can be expressed mathematically:

$$\beta = \frac{L_B}{\lambda} \tag{4.1}$$

where L_B is the beat length where at which the phase difference between the fast and slow axes approximates 2π and λ is the wavelength. The loop mirror provides a periodic filtering effect and the spacing between the constructive wavelength peaks. Therefore, the comb spacing is given by (Lee et al., 2004):

$$\Delta\lambda = \left(\frac{\lambda^2}{\beta L_{pmf}}\right) \tag{4.2}$$

where λ is the peak wavelength of the spacing, β is the birefringence of the PMF and L_{pmf} is the length of PMF. The total phase difference between the two modes can be expressed as (Katz & Sintov, 2008):

$$\emptyset = \frac{2\pi}{\lambda}\beta L_{pmf} \tag{4.3}$$

The transmitted spectrum will travel away from the Sagnac loop and light source, while the reflected spectrum will travel away from the Sagnac loop towards the light source. The transmission spectrum of the SLM is a sinusoidal periodic function to the wavelength and can be given as (Lee et al., 2004):

$$T = sin\frac{\beta L}{\lambda}\cos(\theta_1 + \theta_2) \tag{4.4}$$

Figure 4.2 shows the Sagnac loop mirror (SLM) transmission spectra for different lengths of PMF used in this work, which consists of 2.0 m, 1.0m and 0.5 m long PMF. The transmission spectra for the different PMF lengths are combined in a single graph for comparison purpose. As shown in the figure, the SLM spectra are in the form of comb-like structure with different spacing for different lengths of the PMF used. This characterization of the SLM transmission spectrum is carried out by connecting the input port of the 3 dB coupler in Figure 4.1 to an ASE source whereas the output port of the coupler is connected to an optical spectrum analyser (OSA Yokogawa AQ63703). The obtained results as shown in Figure 4.2 indicates that the comb spacing of the SLM transmission spectrum can be adjusted by varying the length of PMF. The measured optical comb spacing for 0.5 m, 1.0 m and 2.0 m PMF are 16.8 nm, 14.4 nm and 2.4 nm respectively. These experimental values agree well with the estimated values from Equation 4.2. From both the experimental and estimated values, it can be deduced that the comb spacing decreases as the length of the PMF length is increased.

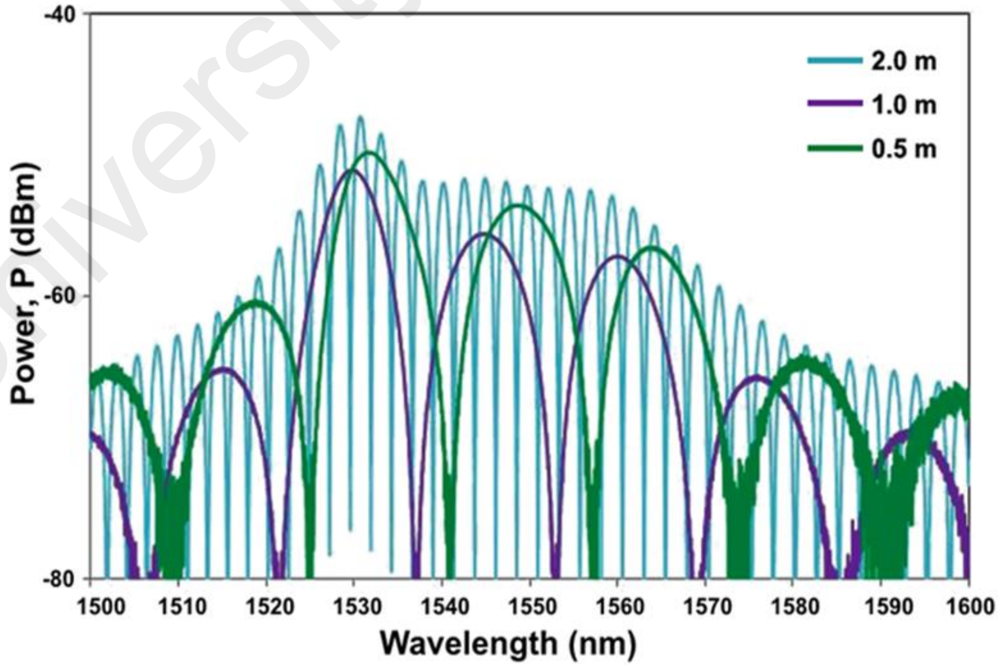

Figure 4.2: SLM output spectrum for 0.5 m, 1.0 m and 2.0 m PMF

The output of the mode-locked spectrum is shown in Figure 4.3 (a)-(c), with different bandwidths obtained by using different lengths of the PMF. The spectral profile of the mode-locked laser obtained by using 0.5 m, 1.0 m and 2.0 m of PMF as shown in Figure 4.3 (a), (b) and (c) respectively and 3 dB bandwidth of the spectral are ~6.0 nm, ~4.0 nm and ~1.0 nm as the average of the dual-wavelength respectively. The centre wavelengths of the mode-locked spectrum for 0.5 m and 1.0 m PMF are ~1563 nm and 1562 nm respectively, as shown in Figure 4.3(a) and 4(b). As in the case of 2.0 m PMF as shown in Figure 4.3(c), a dual wavelength mode-locked output is obtained, with the centre wavelengths of 1557 nm and 1559 nm for the first and second peak respectively. The centre wavelength of each of the generated mode-locked spectrum can be tuned from between 1530 nm to 1560 nm by adjusting the PC, giving the system a tuning range of approximately 30 nm. The average output power of this proposed system is measured to be in the range of ~0.15 to ~0.50 mW.

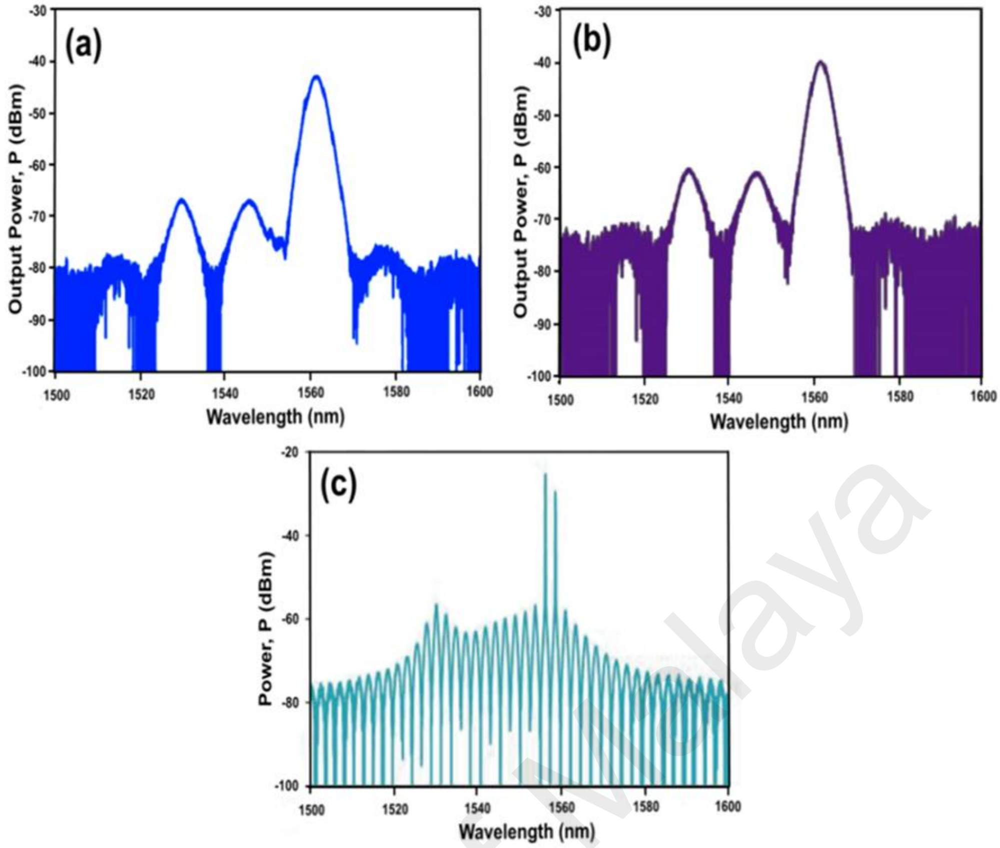

Figure 4.3: Mode-locked spectrum obtained by using a) 0.5m b) 1.0m and c) 2.0m PMF

Figure 4.4 (a)-(c) shows the output pulse train of the proposed system as observed from the oscilloscope. The repetition rate obtained is 12.1 MHz by using 0.5 m PMF, as shown in Figure 4.4 (a), 11.7 MHz by using 1.0 m PMF, as shown in Figure 4.4 (b), and 10.2 MHz by using 2.0 m PMF, as shown in Figure 4.4 (c). These mode-locked pulses operate in the single-pulse regime, matching the round-trip time of the cavity where the single pulse means single pulse traveling back and forth inside the cavity. Every time this pulse reaches the output coupler, the laser emits a part of this pulse. The pulse repetition rate is determined by the time it takes the pulse to make one trip around the cavity. As shown in Equation 4.5, the repetition rate is closely related to the cavity length, L. Based on this equation, it can be deduced that the pulse repetition rate is inversely proportional to the length of the PMF. This augers well with the results obtained in this work.

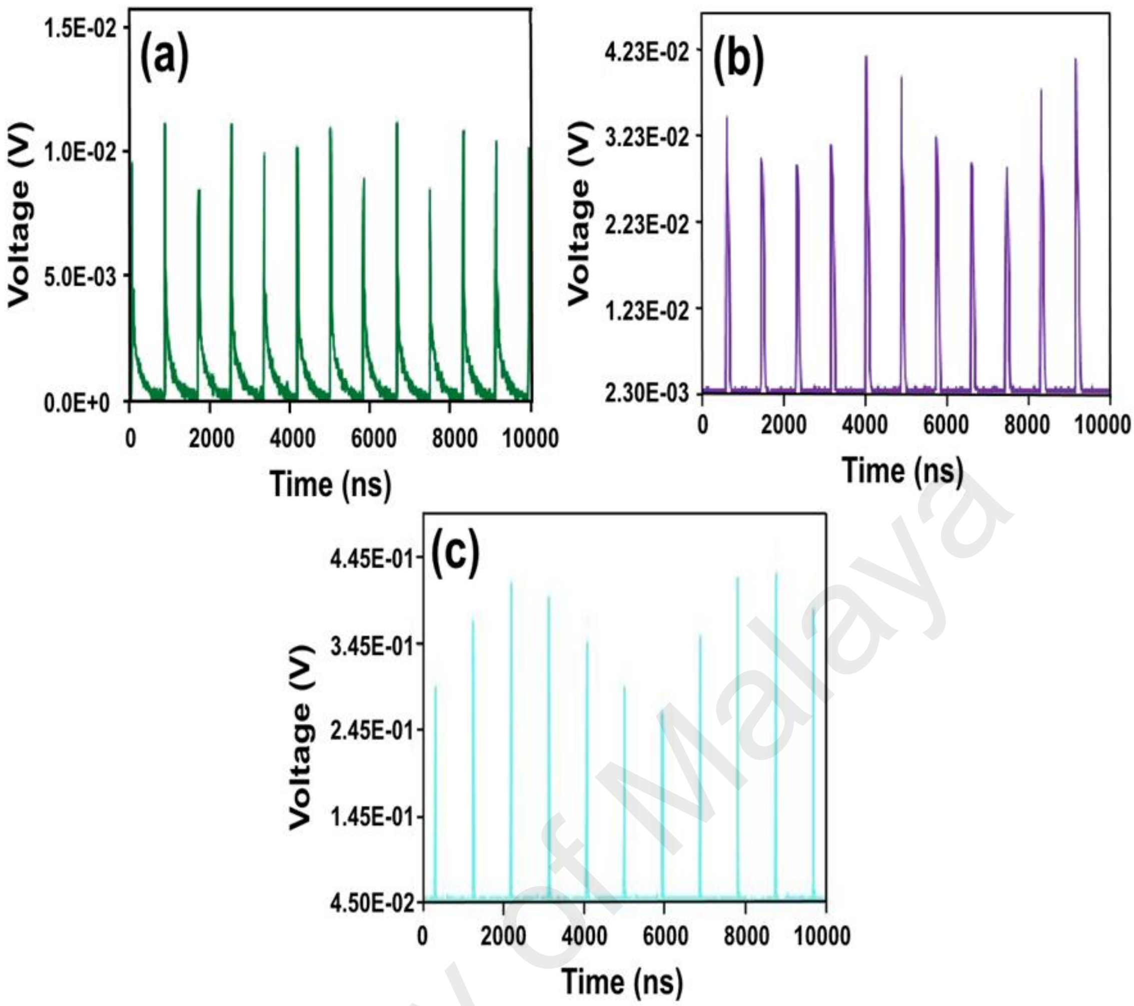

Figure 4.4: Output pulse train obtained using a) 0.5 m b) 1.0 m and c) 2.0 m PMF

$$f_{rep} = \frac{c}{nL} \tag{4.5}$$

where n =1.46 which is the refractive index of silica glass fiber, c is speed of light and L is the cavity length of the ring fiber laser.

Figure 4.5 (a)-(c) shows the autocorrelation trace of the mode-locked output as measured using the autocorrelator for the different lengths of PMF. The estimated pulse widths at the full-widths at half-maximum (FWHM) point for 0.5 m PMF is 0.52 ps, as shown in Figure 4.5 (a). The pulse width increases to 0.75 ps as the length of the PMF is changed to 1.0 m, as shown in Figure 4.5(b). As the length of the PMF is changed to 2.0 m, the pulse width is further increased to 1.65 ps. The pulse widths are dependent on the bandwidth of the mode-locked output spectrum, as indicated by Equation 4.6. The bandwidth of the mode-locked output spectrum, on the other hand, is consequently influenced by the comb spacing of the Sagnac loop. Once a stable mode-locked pulse is achieved, the pulse width remain unchanged even the pump power was increased. This is because the nonlinear dispersion of the cavity was fixed. Thus, when there were change in PMF length the nonlinear dispersion of the cavity change and generate different repetition rate. The time-bandwidth products (TBP) of the proposed system as estimated from Equation 4.6 are 0.37, 0.39 and 0.41 for 0.5 m, 1.0 m and 2.0 m PMF respectively. The TBP values are larger than the transform limited pulse of 0.315 due to some minor chirping (Katz & Sintov, 2008). In Figure 4.5 (c), there is some background noise observed in the experimental trace. This could probably be due to the timing jitter of the mode-locked pulses. This phenomenon is also observed in (Xie et al., 2008) study.

$$TBP= \Delta t \times \Delta v \tag{4.6}$$

where Δt is the pulse width at FWHM in time domain and Δv is the spectral width at FWHM in frequency domain.

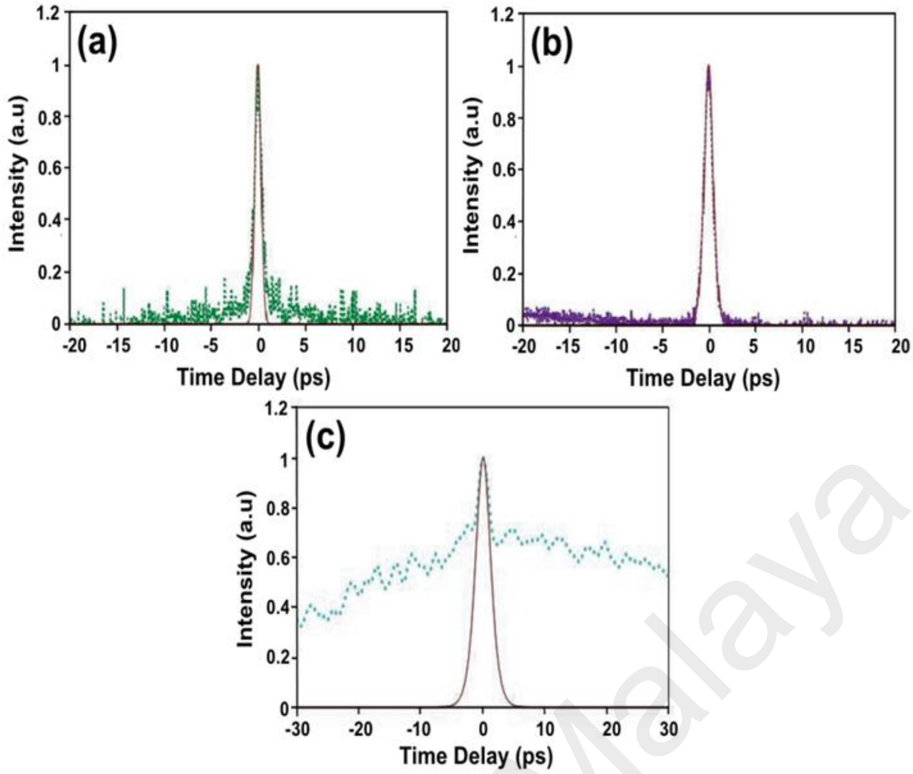

Figure 4.5: Pulse width recorded from the autocorrelation trace for PMF length of a) 0.5 m, b) 1.0 m and c) 2.0 m

To investigate the operation stability of the mode-locked pulses, the RF spectrum of the laser output is measured by using the RFSA. Figure 4.6 (a)-(c) shows the output laser in the frequency domain as obtained from the RFSA for the different lengths of PMF. By using 0.5 m PMF, the first harmonic of the RF spectrum is obtained at 12.1 MHz, as can be seen from Figure 4.6 (a). On the other hand, the first harmonic of the RF spectrum obtained by using 1.0 m PMF is 11.7 MHz, as can be seen from Figure 4.6(b). As for the 2.0 m PMF, the first harmonic of the RF spectrum is observed at 10.2 MHz, as can be seen in Figure 4.6 (c). The subsequent harmonics of the RF spectrum occur at n^{th} intervals for all the three cases, thus validating the pulse train obtained in Figure 4.4 (a)-(c).The spectrum of subsequent harmonics is at consistent RF interval, as is to be expected. The even spacing of the harmonics also verifies that there are no Q-switching instabilities in the mode-locked pulses and proves that the spectrum is free from spectral modulation (Ahmad et al., 2012) which is also indicated by the output pulse train shown in Figure 4.4.

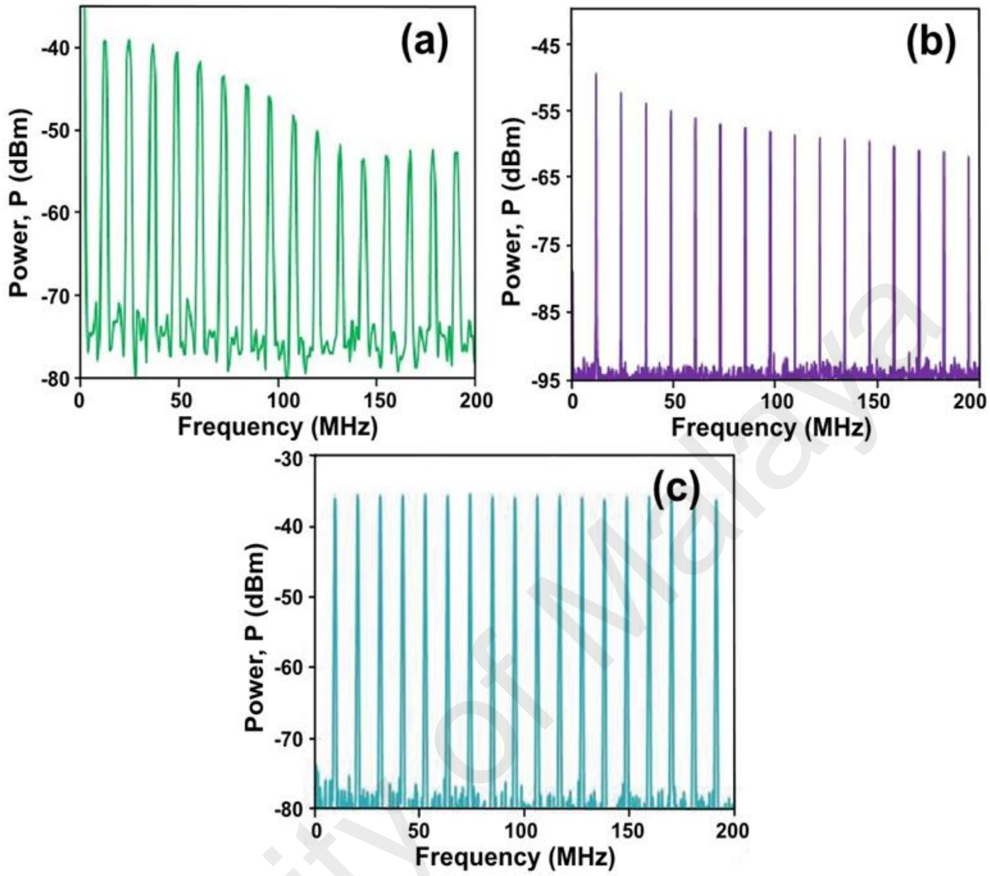

Figure 4.6: RF spectrum of the output pulse for a) 0.5m, b) 1.0m and c) 2.0 m of PMF

4.2 Switchable dual-wavelength in passively Q-switched fiber laser by using AWG

Stable dual-wavelength Q-switched pulsed laser with variable wavelength separation is obtained from this proposed system, as shown in Figure 4.7 (a–d). Type of laser mode generated from this experiment is different from the previous experiment even though same SA was used. This is due to the implementation of filter in the laser cavity. The filter helps in filtering the wavelengths thus indirectly made the spectrum bandwidth narrower. As has been discuss earlier repetition rate closely related with the spectrum bandwidth.

Two channels from the AWG are selected and combined to generate the dual wavelength fiber laser, such that one wavelength is fixed at 1530.5 nm using the first channel of the AWG, and the other wavelength is obtained from another channel of the AWG. As the channels of the AWG can be switched, different wavelength spacing of the dual-wavelength output can be obtained, which ranges from 1.6 to 4.0 nm. By combining the first and second channel of the AWG, a dual wavelength laser with a wavelength spacing of 1.6 nm is obtained.

In this case, CW laser threshold of the dual-wavelength operation is reached at pump power of about 12.4 mW. Once the pump power exceeds 22.4 mW, Q-switching behavior is observed. The output spectrum of the dual wavelength Q-switched fiber laser with the wavelength separation of 1.6 nm taken at pump power of 141.3 mW is shown in Figure 4.7 (a), with the output wavelengths at 1530.5 and 1532.1 nm. By switching the second channel to the third channel, the wavelength spacing can be increased to 2.4 nm, giving the output wavelengths of 1530.5 and 1532.9 nm, respectively, as shown in Figure 4.7 (b). By further switching the channel to fourth and fifth channel results in further increase in the wavelength spacing, as shown in Figure

4.7 (c, d) respectively, with the respective value of 3.2 and 4.0 nm. This corresponds to the output wavelengths of 1533.7 and 1534.5 nm for the second wavelengths.

Figure 4.8 shows the repetition rate of the dual-wavelength Q-switched pulsed laser against pump power for different wavelength spacing of 1.6, 2.4, 3.2 and 4.0 nm which are combined in a single graph for comparison purpose. Overall, for all the four different wavelength spacing, the repetition rate increases almost linearly with the pump power. From the graph, it can be seen that as in the case of wavelength spacing of 1.6 nm, the repetition rate starts from 26.4 kHz at the pump power of ~22.4 mW, which is the Q-switching threshold, to a maximum repetition rate of 54.9 kHz at the pump power of ~141.3 mW, with an increase rate of approximately 2–5 kHz for every increase of 10 mW in the pump power. As for the wavelength spacing of 2.4 nm, the repetition rate starts from 23.14 kHz at the pump power of ~22.4 mW to a maximum repetition rate of 51.6 kHz at the pump power of ~141.3 mW, with an increase rate of approximately 2–5 kHz for every increase of 10 mW in the pump power. For the wavelength spacing of 3.2 nm, the repetition rate starts from 19.5 kHz at the pump power of ~22.4 mW to a maximum repetition rate of 48.2 kHz at the pump power of ~141.3 mW, with an increase rate of approximately 2–5 kHz for every increase of 10 mW in the pump power.

On the other hand, for the wavelength spacing of 4.0 nm, the repetition rate starts from 12.2 kHz at the pump power of ~22.4 mW to a maximum repetition rate of 40.7 kHz at the pump power of ~141.3 mW, with an increase rate of approximately 2–4 kHz for every increase of 10 mW in the pump power. It is expected that a higher repetition rate can be obtained by further increasing the pump power above 141 mW, but the laser pump used in this work limits this. In contrast to the repetition rate behavior against the pump power, the pulse width decreases with the increase of the pump power.

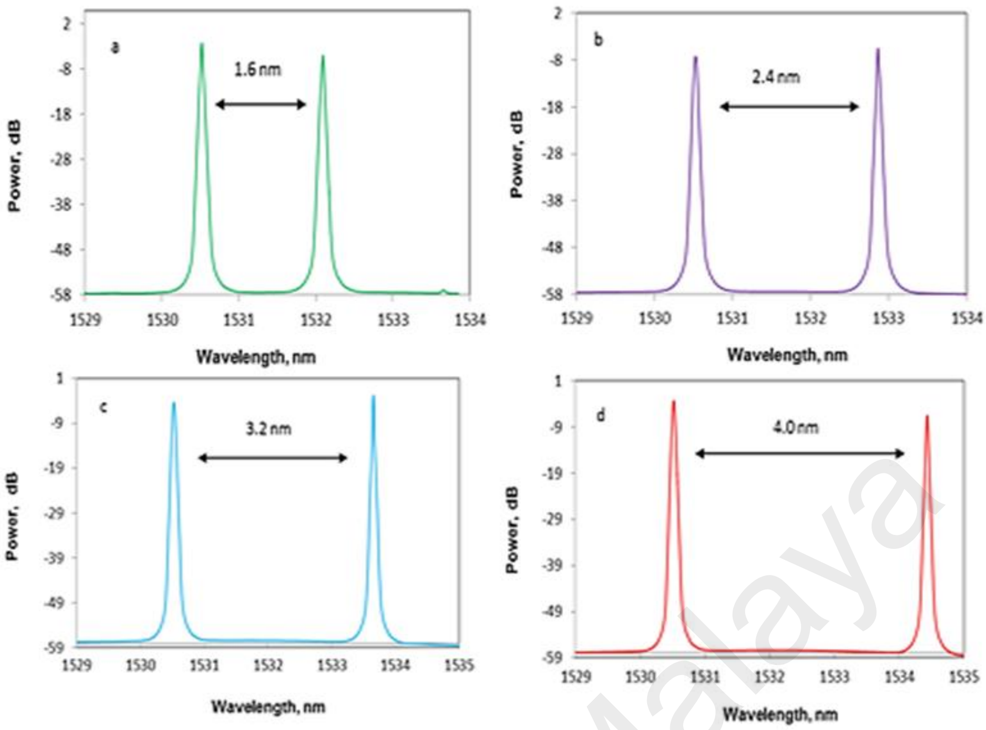

Figure 4.7: Stable dual-wavelength Q-switched pulsed laser with variable wavelength separation

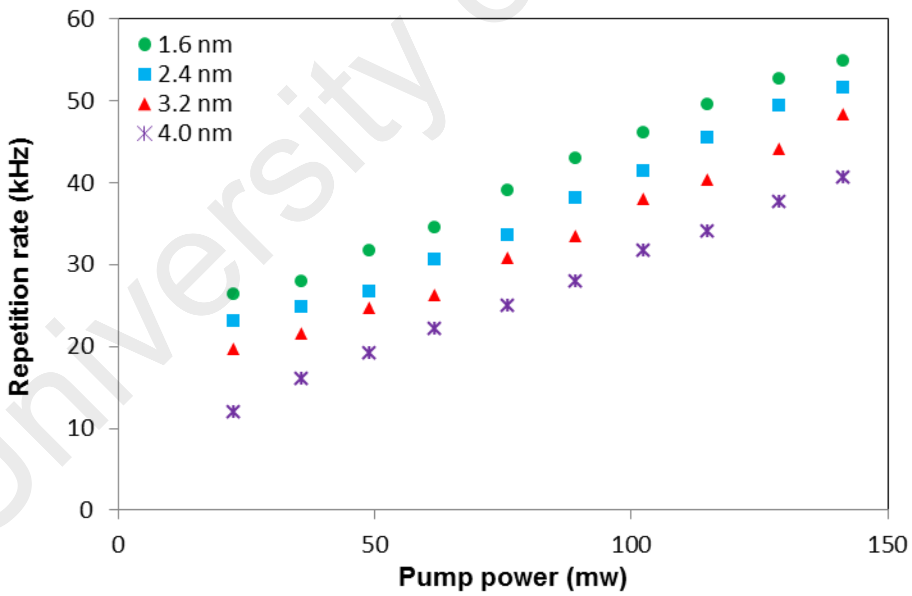

Figure 4.8: Repetition rate of the dual-wavelength Q-switched pulse against pump power for different wavelength spacing of 1.6, 2.4, 3.2 and 4.0 nm

Figure 4.9 shows the combined graph of the output pulse width against the pump power for the different wavelength spacing. Among all the plotted graphs, the graph corresponding to the wavelength spacing of 1.6 nm gives the narrowest average pulse width value, with the pulse width decreasing from a value of 2.8–0.9 μs as the pump power is increased from ~22.4 to ~141.3 mW, followed by the wavelength spacing of 2.4, 3.2, and 4.0 nm, with their respective narrowest pulse width of 1.1, 1.4, and 2.3 μs. It is interesting to observe that the pulse width value is interrelated to the wavelength spacing of the output spectrum, whereby a narrower spacing between the two wavelengths will result in a narrower pulse width at any given pump power.

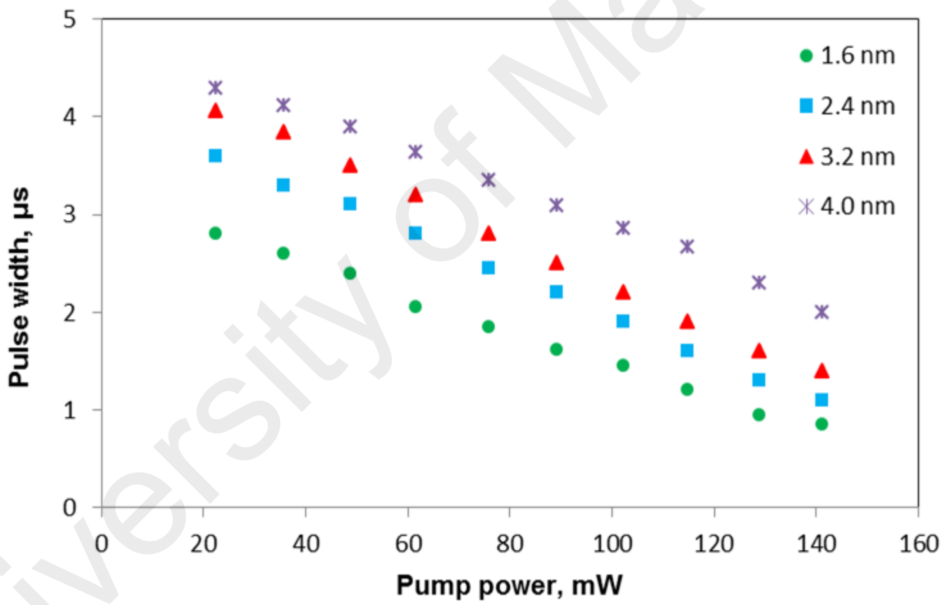

Figure 4.9: Output pulse width against the pump power for the different wavelength spacing

The output pulse train of this dual-wavelength Q-switched fiber laser is shown in Figure 4.10 (a–d), corresponding to the wavelength spacing of 1.6, 2.4, 3.2, and 4.0 nm, respectively, as taken from the oscilloscope trace at the highest pump power of 141.3 mW. The pulse train in Figure 4.10 (a) has a pulse interval of 18.2 μs, giving the repetition rate value of 54.9 kHz. In Figure 4.10 (b), the time interval between the pulses is 19.4 μs, corresponding to the repetition rate value of 51.6 kHz. As for Figure

4.10 (c, d), the pulse interval values are 20.1 and 24.6 μs, respectively, with the respective repetition rate value of 48.2 and 40.7 kHz. As can be seen from all the graphs in Figure 4.8, the Q-switched pulses experience some fluctuations in the Y-axis, which could be attributed to some interactions between the two lasing lines of the dual-wavelength fiber laser, since the output port is common.

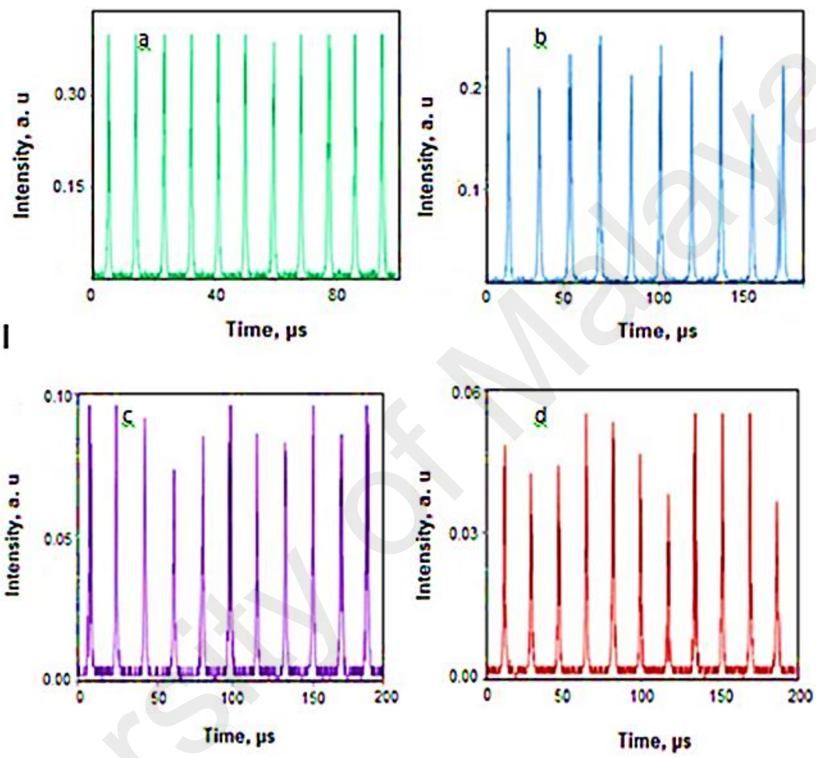

Figure 4.10: Output pulse train dual-wavelength Q-switched fiber laser for wavelength spacing of (a) 1.6, (b) 2.4, (c) 3.2 and (d) 4.0 nm

In comparison with an earlier work by (Luo et al., 2010), the demonstration of dual-wavelength output using graphene has a lower threshold of about 6.5 mw at 974 nm as compared to the above experiment which has a value of 22.4 and 12.4 mW for Q-switched and CW dual-wavelength output. The lower value is primarily due to graphene, which has a lower insertion loss as compared to CNT, and also the usage of fiber Bragg grating to generate the dual wavelength output. As in the case of this work, an arrayed waveguide is used inside the cavity, which has an insertion loss of about 4.5–5.5 dB, and this causes the higher threshold pump power needed for generating the dual-wavelength Q-switched pulse. The advantage of this setup is it allows tunability of the spacing between the two wavelengths that is tuned from 1.6 to 4.0 nm, which can be further extended by choosing different channels of the AWG. The tunability of (Luo et al., 2010) only demonstrates a fixed wavelength spacing which can be tuned as a pair in the wavelength range of 1566 to 1570 nm. Besides the tunable wavelength spacing between them as in the case of this experiment, the tunable pair can also be tuned in the C-band region by choosing the appropriate channels of the AWG, which provides an added advantage.

4.3 Tunable pulse width in passively Q-switched fiber laser by using UNTBF

In this case, the continuous wave (CW) laser threshold was reached at pump power of 15.50 mW. Q-switching behavior was observed once the pump power exceeded 35.50 mW with an average output power of approximately 1.40 μW. The performance of the Q-switched fiber laser output was further investigated for the circumstances of pump power increases from 35.50 mW to 107.20 mW. Figure 4.11 (a) shows the repetition rate and pulse width of the Q-switched fiber laser at a centre wavelength of approximately 1558.85 nm. By increasing the pump power, the repetition rate increased linearly from 7.50 kHz to 22.50 kHz. On the other hand, the pulse width behaved oppositely, whereby the pulse width became narrower as the pump power increased. The lowest pulse width attained was 4.10 μs and the highest pulse width obtained was 13.40 μs. Q-switched pulses became unstable and started to disappear when the pump power exceeded 107.20 mW.

However, the occurrence of Q-switching pulses could be demonstrated again once the pump power dropped below 107.20 mW, which showed that the CNT-based SA had incurred no sustained damage. This SA behavior could be attributed to the influence of the thermal effect on the SA as long as the damage threshold is not exceeded. In light of this restriction, the pump power was limited below an estimated level that could result in a breaching of the damage threshold. As shown in Figure 4.11 (b), an increase in the pump power corresponded to the average output power rising linearly and a linear increase in pulse energy, from 0.11 nJ to 2.05 nJ. The highest average output power gained from the system was 8.40 μW.

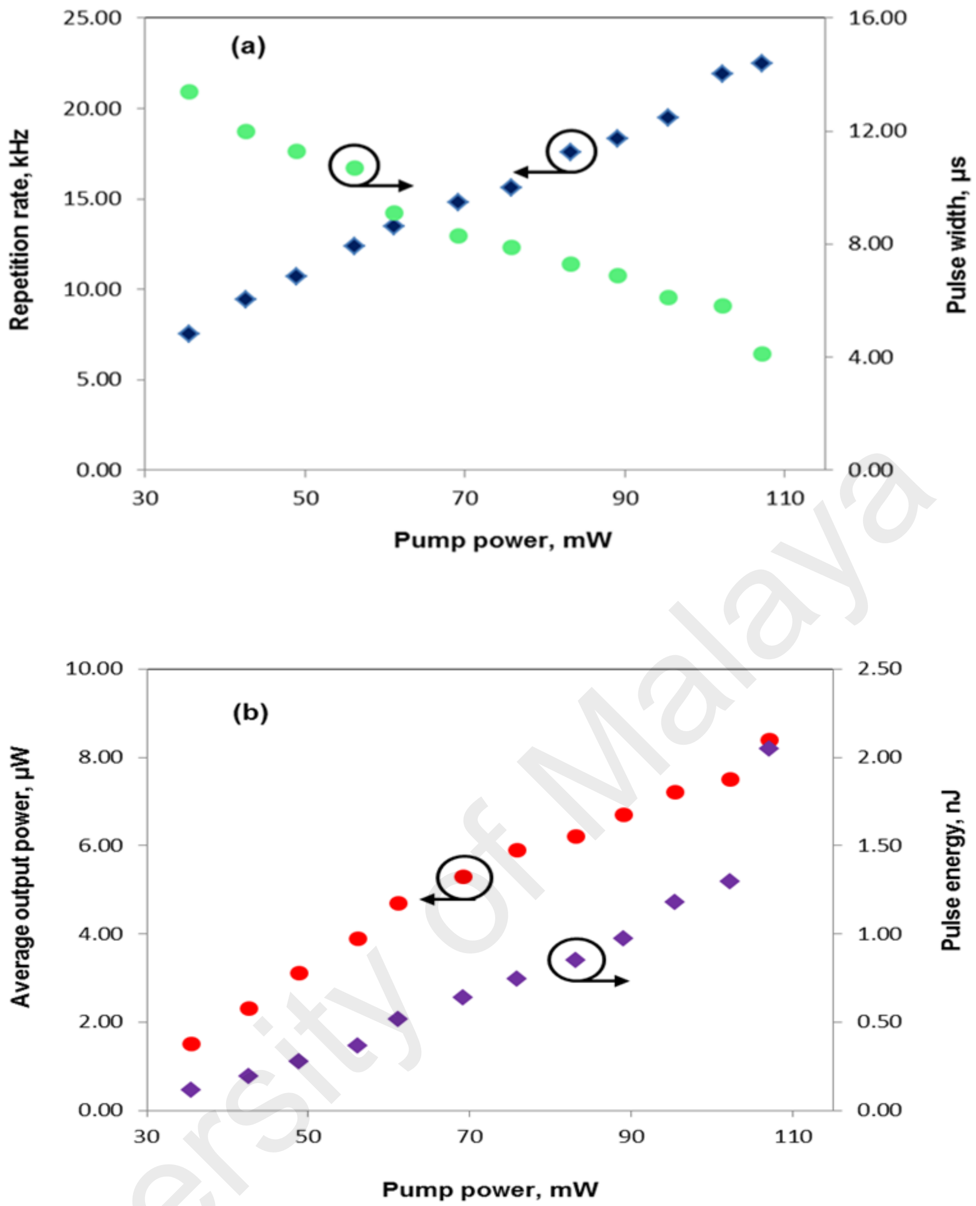

Figure 4.11: a) Repetition rate and the average output power, and b) pulse width and pulse energy, across a range of pump power

The Q-switched fiber laser output pulse trains that corresponded to pump power of 35.50 mW and 107.20 mW are shown in Figure 4.12 (a) and (b) respectively. The pulse train in Figure 4.12 (a) had a pulse interval of 132.80 μs, giving a repetition rate of 7.53 kHz, and in Figure 4.12 (b), the 44.40 μs time interval between pulses corresponded to a repetition rate of 22.53 kHz. Observation of these graphs reveals that the Q-switched pulses experienced fluctuations in intensity, which could be attributed to timing jitter.

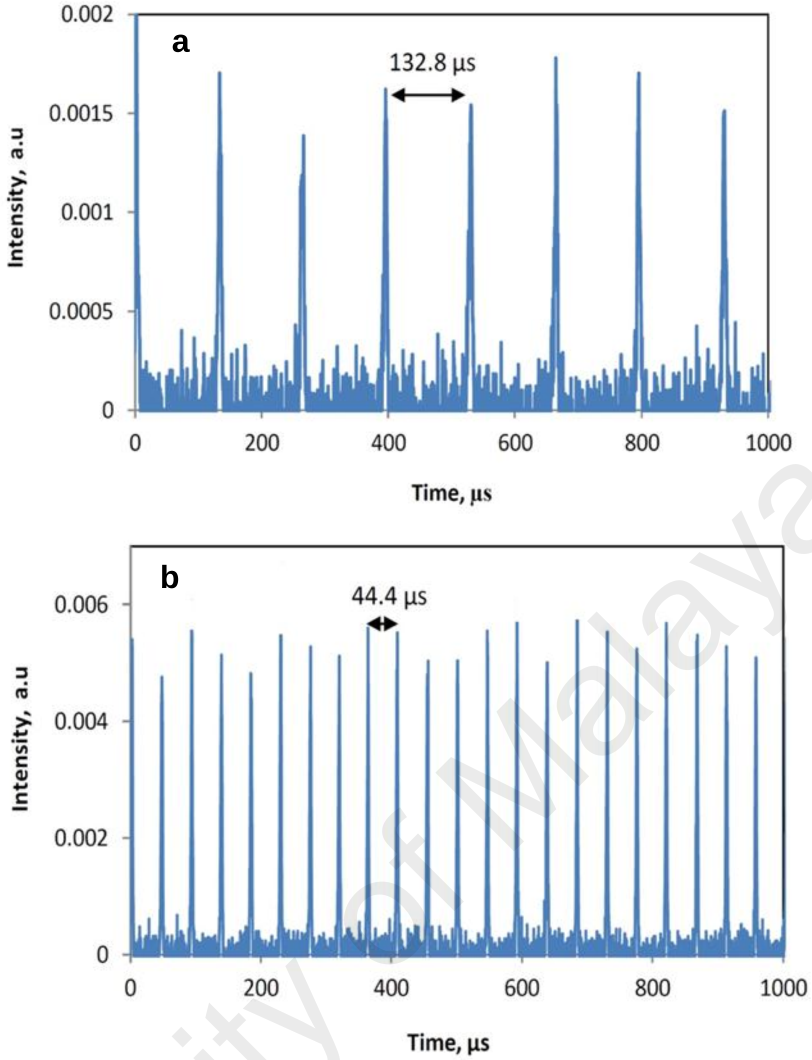

Figure 4.12: Output pulse train of the Q-switched fiber laser at pump power of (a) 35.50 mW, and (b) 107.2 mW

The most favorable aspect of this proposed Q-switched fiber laser system is the capability for varying the pulse energy by controlling the Q-switched spectral bandwidth. Figure 4.13 shows the output of Q-switched spectra with different bandwidths, whereby adjustments to the bandwidth of the tunable bandpass filter were performed while maintaining a pump power of 75.90 mW with a centre wavelength of approximately 1558.85 nm. The 3 dB bandwidth spectra obtained by tuning the filter were 0.48 nm, which is the largest obtainable bandwidth, followed by 0.47 nm, 0.46 nm, 0.43 nm, 0.34 nm, 0.22 nm, 0.14 nm, 0.07 nm, 0.04 nm, and the narrowest bandwidth, 0.02 nm. The profile of the spectrum bandwidth was influenced by the passive bandwidth of the grating built in the tunable bandwidth filter. The passive bandwidth can be expressed mathematically as

$$\Delta\lambda = (d\lambda/\pi\omega m)\cos\alpha \tag{4.7}$$

where d is the groove spacing of the grating, λ is the laser wavelength, ω is the beam radius, m is the diffraction order, and α is the incident angle (Fan et al., 2003).

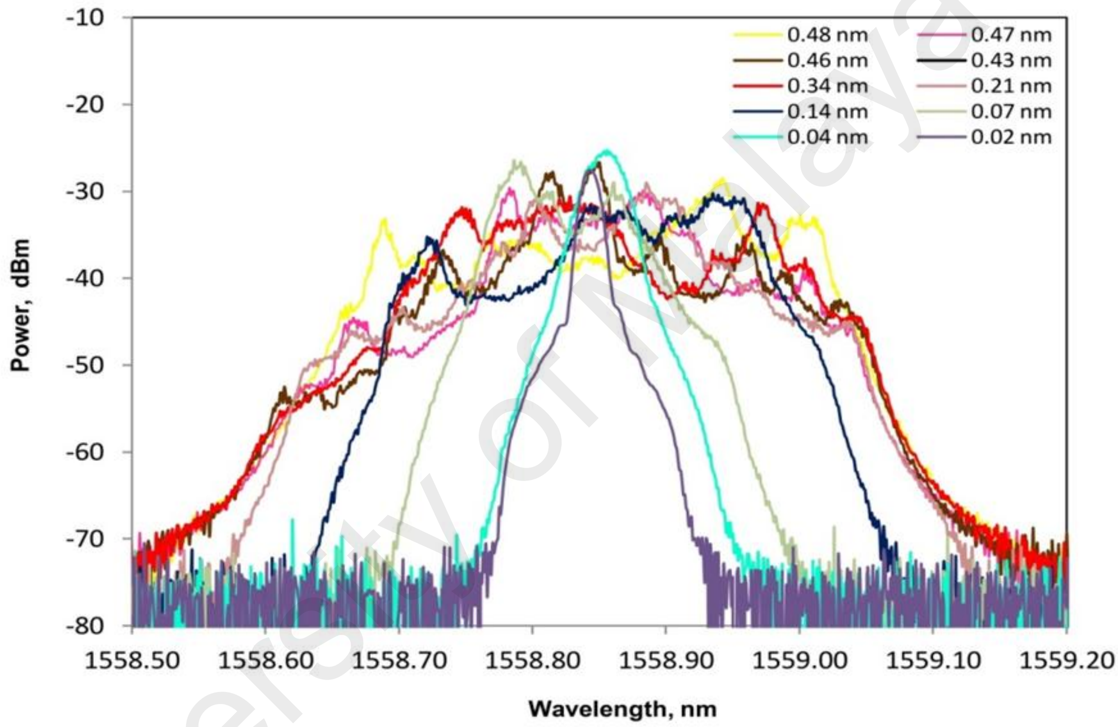

Figure 4.13: Q-switched spectra with different bandwidths at a fixed pump power of 75.9 mW

Figure 4.14 (a) shows the repetition rate and the average output power at a variety of bandwidths while pump power was fixed at 75.90 mW. As observed from the figure, the repetition rate and the average output power increased gradually in accordance with the 3 dB bandwidth of the tunable bandpass filter being varied linearly from 0.02 nm to 0.48 nm. The lowest repetition rate and average output power obtained were 16.23 kHz and 1.67 μW respectively at the narrowest bandwidth, 0.02 nm, and the highest repetition rate and average output power achieved were 26.16 kHz and 1.76 μW respectively at the widest bandwidth, 0.48 nm. These results represent an increase of repetition rate and average output power from about 0.46 to 2.32 kHz, and approximately 0.2 to 0.5 μW respectively.

On the other hand, the behavior of the pulse width with the behavior of the repetition rate, as can be observed in Figure 4.14 (b), is vice versa to the case for Figure 4.14 (a).

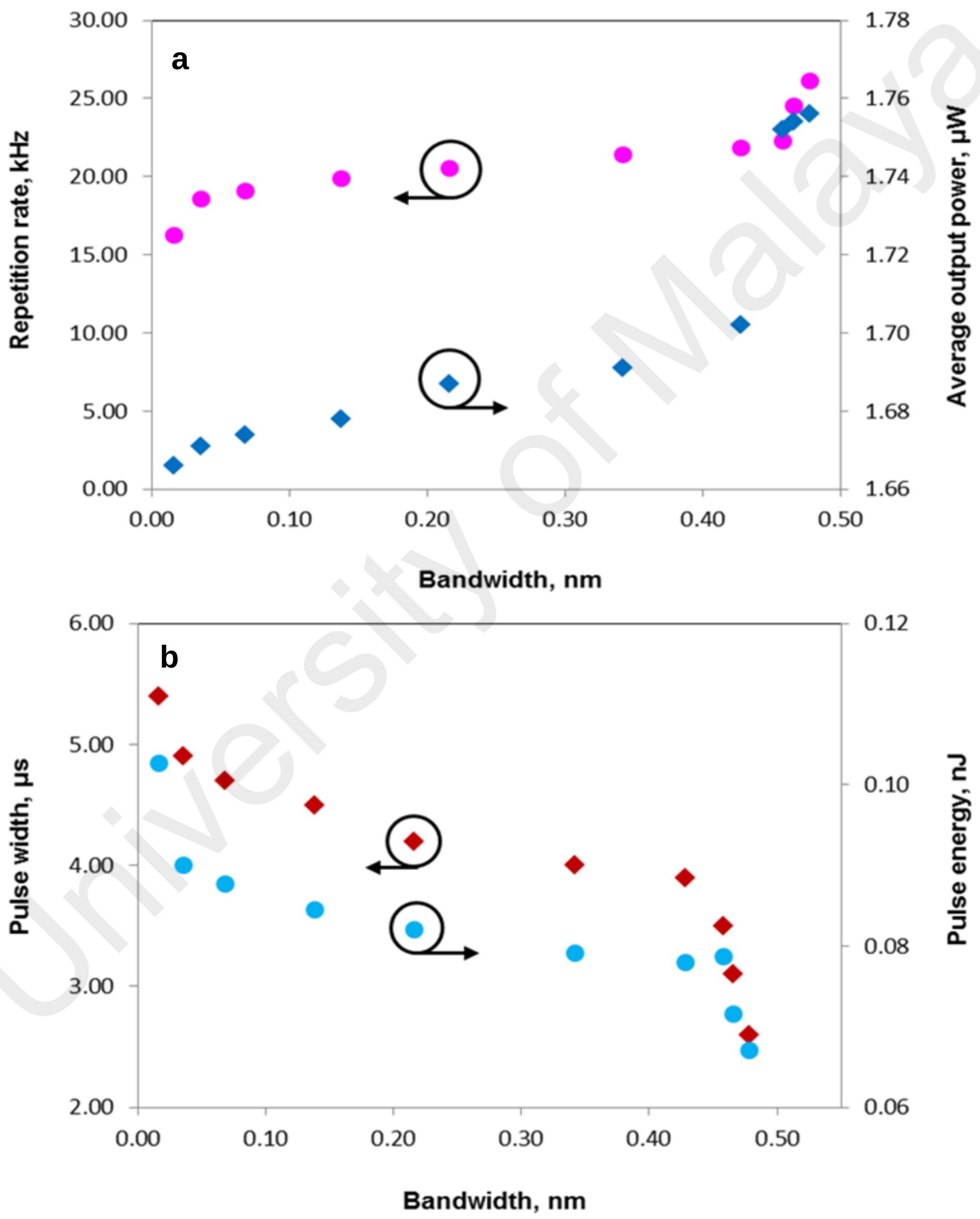

Figure 4.14: The behavior of a) repetition rate and the average output power, and b) pulse width and pulse energy, for different bandwidths

From Figure 4.14 (b), pulse width can be seen to decrease gradually as the bandwidth of the Q-switched spectrum widened. The shortest pulse width was 2.60 μs at the widest bandwidth, 0.48 nm, and the longest pulse width achieved was 5.40 μs at the narrowest bandwidth, 0.02 nm. Pulse energy could be obtained by dividing average output power with the repetition rate of the pulse laser. The pulse energy at fixed pump power 75.9 mW and different bandwidths is shown in Figure 4.14 (b). Pulse energy, as with the case of pulse width, was observed to decrease gradually when the bandwidth became wider. Pulse energy was closely related with repetition rate, and in this case, the repetition rate obtained was influenced by the pulse width achieved via controlling the bandwidth. Therefore, the lowest pulse energy obtained was 0.06 nJ at a spectrum bandwidth of 0.48 nm and the highest pulse energy achieved was 0.10 μJ at a spectrum bandwidth of 0.02 nm.

Figure 4.15(a) and (b) display the output pulse trains of this passively Q-switched erbium-doped fiber laser at a pump power of 75.9 mW for shortest pulse width and longest pulse width respectively, as taken from the oscilloscope trace. The pulse train in Figure 4.15 (a) has a pulse interval of 38.20 μs, giving a repetition rate value of 26.16 kHz. In Figure 4.15 (b), the observed time interval between the pulses is 61.60 μs, corresponding to a repetition rate value of 16.20 kHz. As can be seen from both graphs in Figure 4.15, the Q-switched pulses experienced only very small fluctuations in intensity which the biggest fluctuations are approximately 0.0002 a. u and 0.0005 a. u for 2.6 μs pulse and 5.40 μs pulse width respectively. This shows that the Q-switched pulses are stable at a pump power of 75.9 mW.

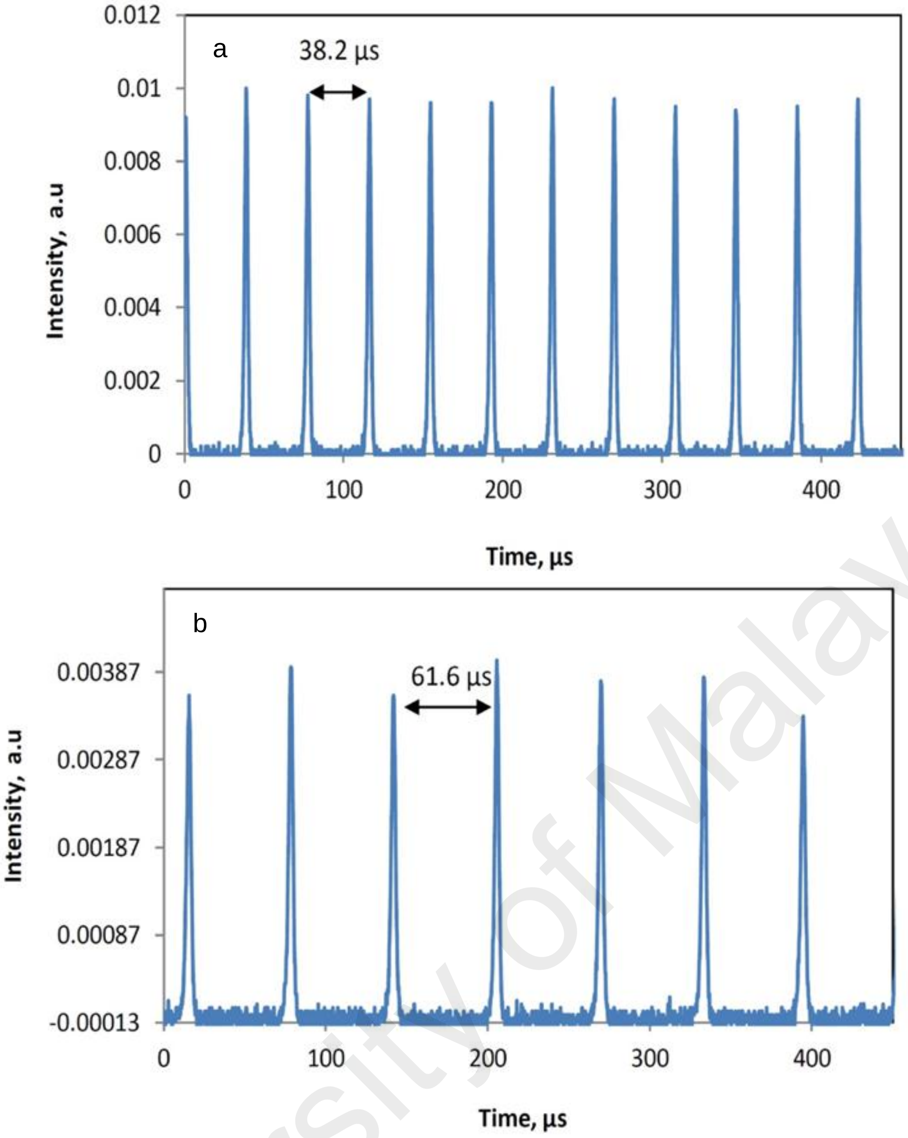

Figure 4.15: Output pulse train of passively Q-switched erbium-doped fiber at a pump power of 75.90 mW, with pulse width of a) 2.60 µs, and b) 5.40 µs

4.4 Tunable ultra-narrow linewidth in passively Q-switched fiber laser by using UNTBF

In this experiment, ultra-narrow linewidth laser is demonstrated by employing an ultra-narrow TBF. Figure 4.16 (a) shows a continuous wave (CW) laser from the ring cavity without the insertion of the ultra-narrow TBF, whereas Figure 4.16 (b) is the ultra-narrow linewidth laser spectrum achieved with the use of ultra-narrow TBF. Both spectra are taken at 100 nm wavelength span and the resolution is fixed to 0.02 nm at a pump power of 83.2 mW. As depicted in the figure, the ultra-narrow linewidth laser spectrum is represented by a very sharp thin line at the centre wavelength of 1561 nm and a 3 dB bandwidth of 0.013nm. On the other hand, the free run laser attained without the use of the ultra-narrow TBF has a centre wavelength of 1567.85 nm with wider 3 dB bandwidth of 0.341 nm.

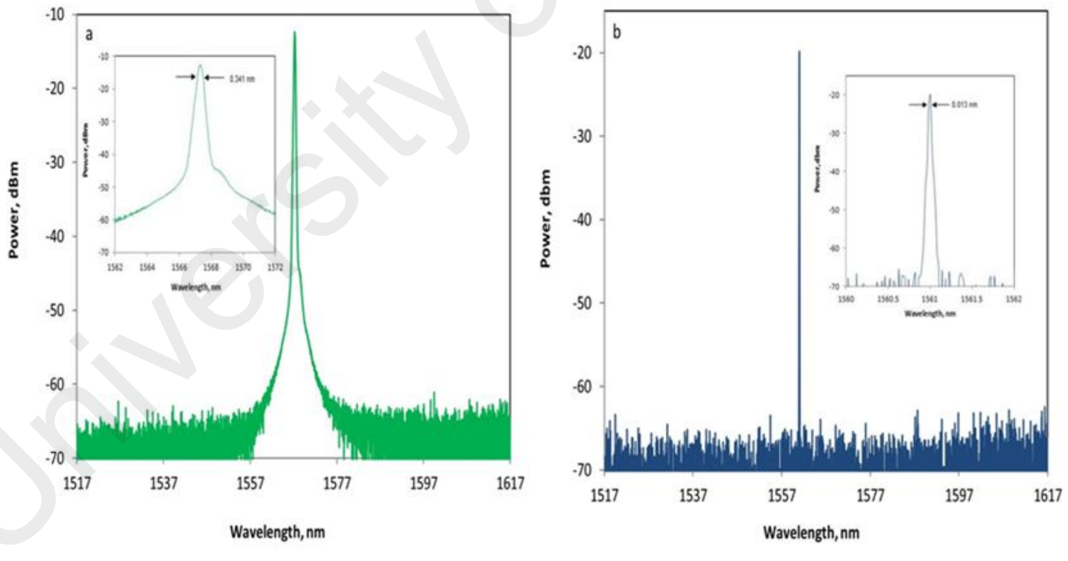

Figure 4.16: (a) normal continuous wave (CW) laser without UNTBF and (b) the narrow linewidth laser spectrum by employing UNTBF

Single longitudinal mode (SLM) is one of the factors that can contribute to a narrow linewidth laser. In order to verify whether the CW laser is operating in SLM, further investigation is carried out. Figure 4.17 shows the laser output as observed from the radio frequency spectrum analyzer (RFSA) across a frequency span of 0–500 MHz. From the observation, the absence of beat frequency verifies that the laser is operating in SLM. Further verification of the SLM operation is done by heterodyned technique using a local oscillator. The output spectrum obtained from the RFSA is shown in Figure 4.18, whereby the presence of a beat signal at 44.80 MHz is detected. The bandwidth of the beat signal, Δf_b was taken at 20-dB point to avoid any frequency jitter. Then, we could relate Δf_b with laser linewidth, Δv, by $\Delta f_b = 2\sqrt{99}\,\Delta v$. Therefore, from the measurement and calculation, the laser linewidth frequency is estimated to be 17.5 kHz which is smaller than what has been reported in (Zhu & Huang, 2014) study. This value proves that the laser operates in SLM as the value is in kilohertz range.

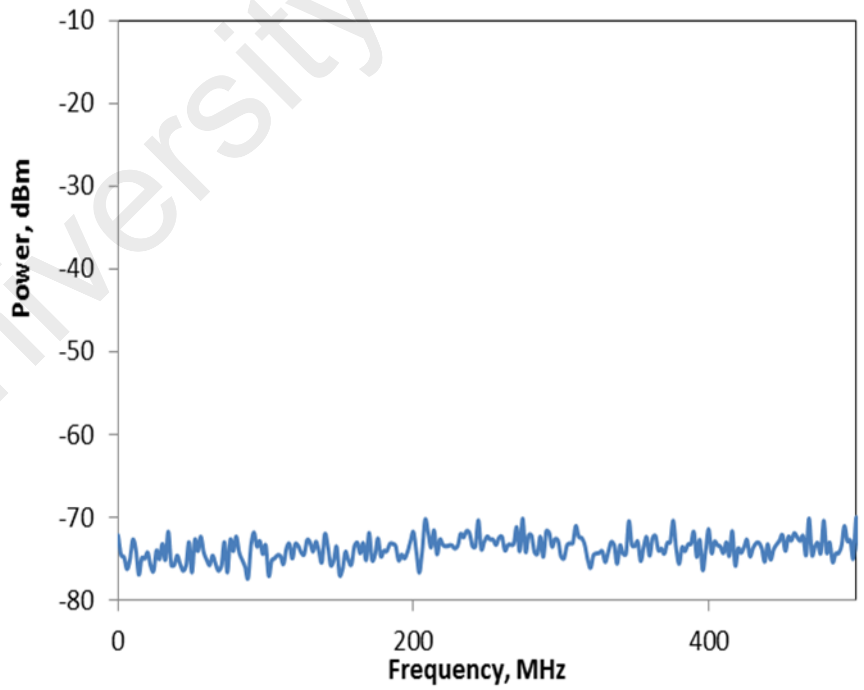

Figure 4.17: Figure 4.17: The laser output as observed from the RFSA across an approximate 0–500 MHz frequency span

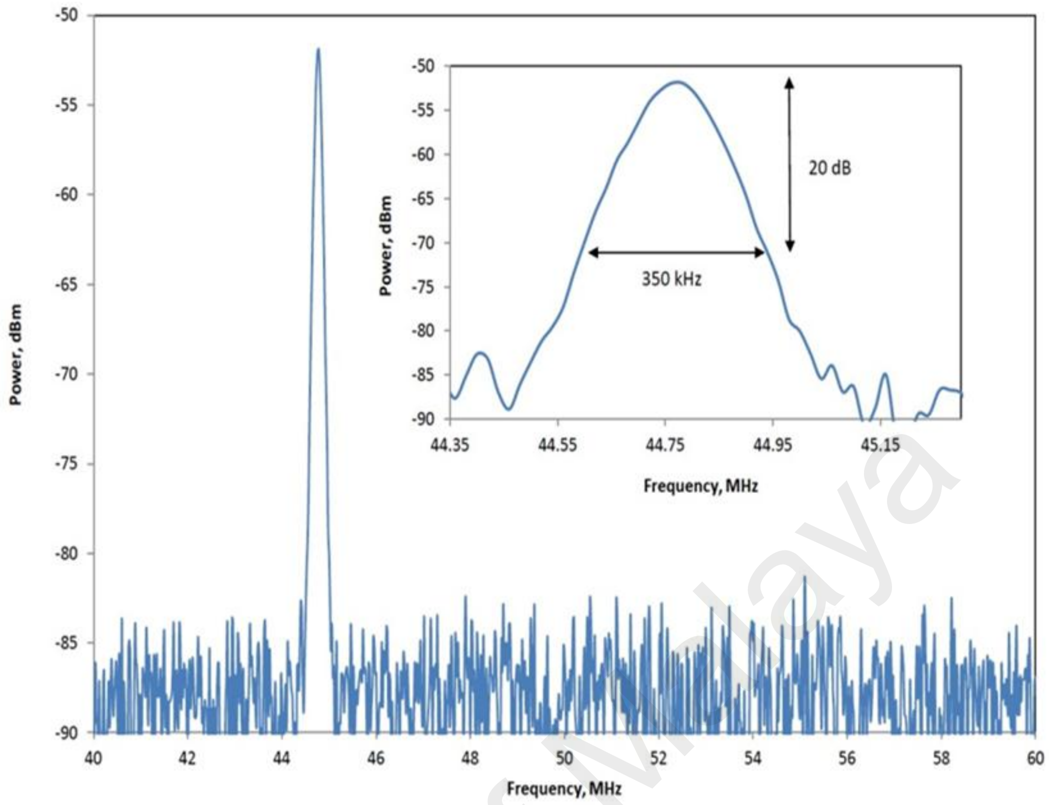

Figure 4.18: RF spectrum of delayed self-heterodyne signal

The ultra-narrow linewidth continuous wave (CW) operation starts at a pump power of 42.7 mW, while the threshold pump power for ultra-narrow linewidth in the Q-switched mode starts at 52.4 mW. Figure 4.19 shows the ultra-narrow linewidth of the Q-switched spectrum at a centre wavelength of 1561.0 nm with the pump power of 83.2 mW, resulting to 3.14 μW of average output power. As shown in the figure, the bandwidth of the Q-switched spectrum is very narrow, with a 3 dB bandwidth of approximately 0.017 nm.

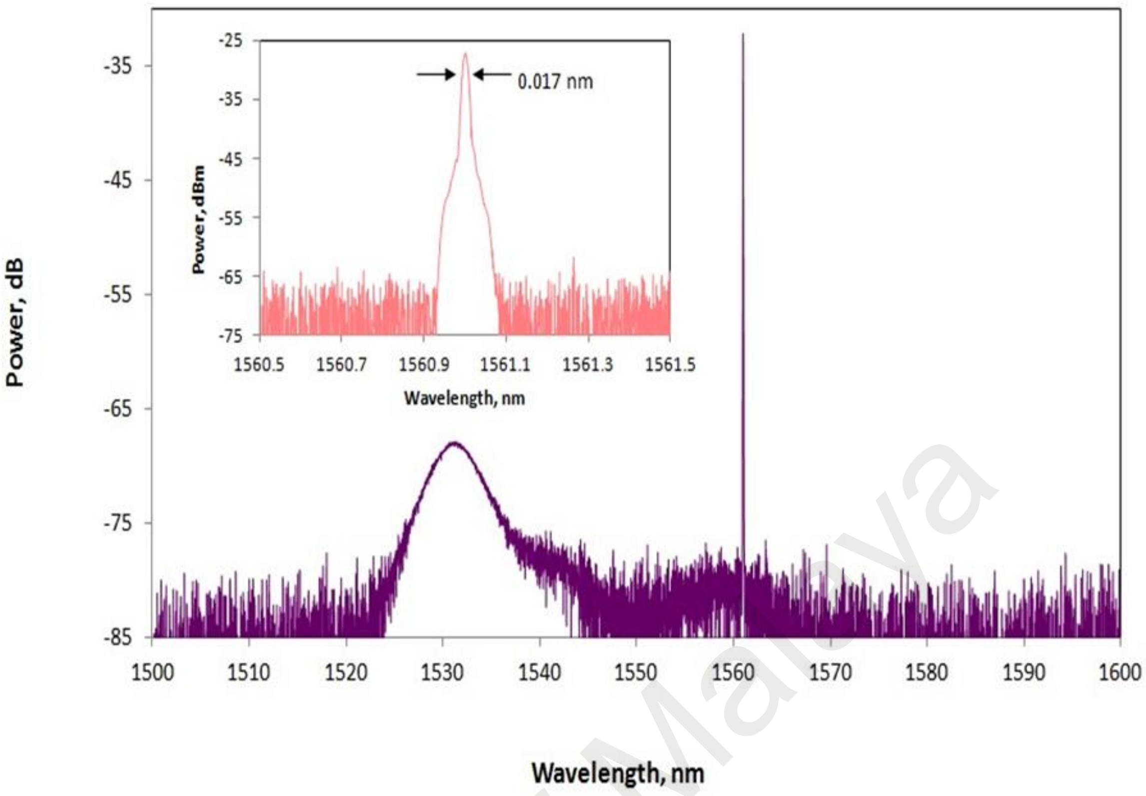

Figure 4.19: Ultra-narrow linewidth of Q-switched spectrum at centre wavelength 1561.0 nm

To further investigate the performance of the ultra-narrow linewidth Q-switched laser, the pump power is varied from 52.4 mW to 83.2 mW. The Q-switched pulses became unstable as the pump power is increased higher than 83.2 mW which might be a result from the CNT-based SA becoming saturated. Therefore, the value of pump power is limited within the optimal Q-switched operating range. The repetition rate and pulse width behaviour as the pump power is varied is shown in Figure 4.20. From the figure, the repetition rate increases as the pump power is raised and the highest repetition rate attained is 23.41 kHz at the pump power of 83.2 mW. As in a typical Q-switched operation, the pulse width gets narrower as the pump power is increased. The smallest pulse width obtained is 2.04 μs at the highest pump power which corresponds to the highest repetition rate.

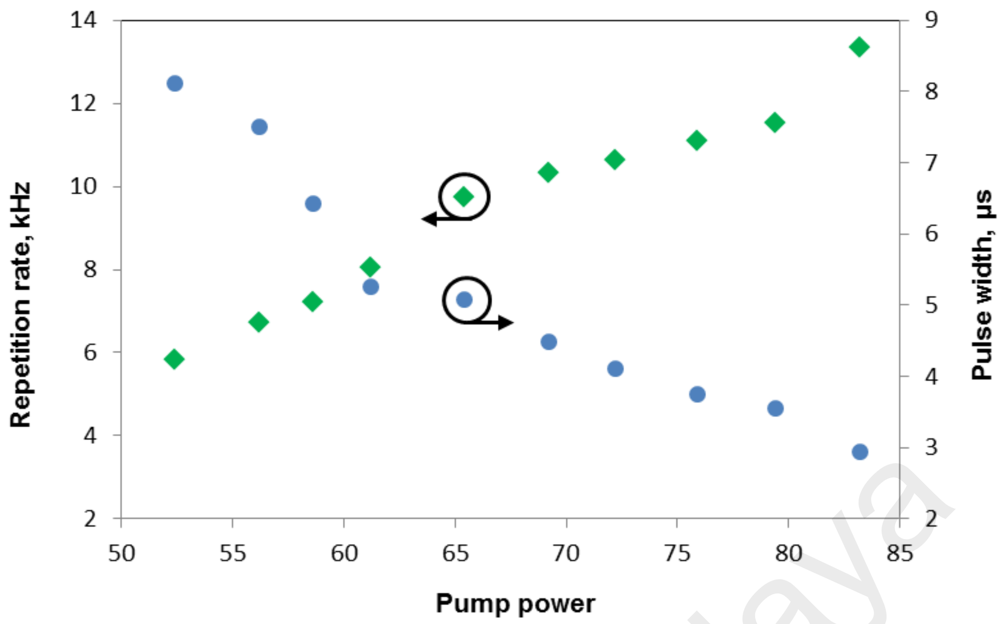

Figure 4.20: The behavior of repetition rate and pulse width as the pump power is varied

The variation of the average output power and pulse energy as the pump power increases from 52.4 mW to 83.2 mW is demonstrated as in Figure 4.21. From the figure, average output power increases almost linearly as the pump power increases. The increment of average output power is in the range of 0.11 to 0.28 µW and the highest output power achieved is 2.51 µW. Most of the losses in this cavity is contributed by the ultra-narrow TBF, causing loss of approximately 20 dB. Pulse energy could be obtained by dividing the average output power with the repetition rate and from the figure, the pulse energy increases as the pump power increases.

The most interesting part of these experiments is the ultra-narrow linewidth of Q-switched laser, which is tunable from 1525 nm to 1561 nm which is about 37 nm in range as shown in Figure 4.22. The Q-switched spectra were tuned at fixed pump power, 83.2 mW with the average 3 dB bandwidth of the Q-switched spectrum is approximately 0.017 nm which is narrower than what have been reported in (Fan et al., 2003) study.

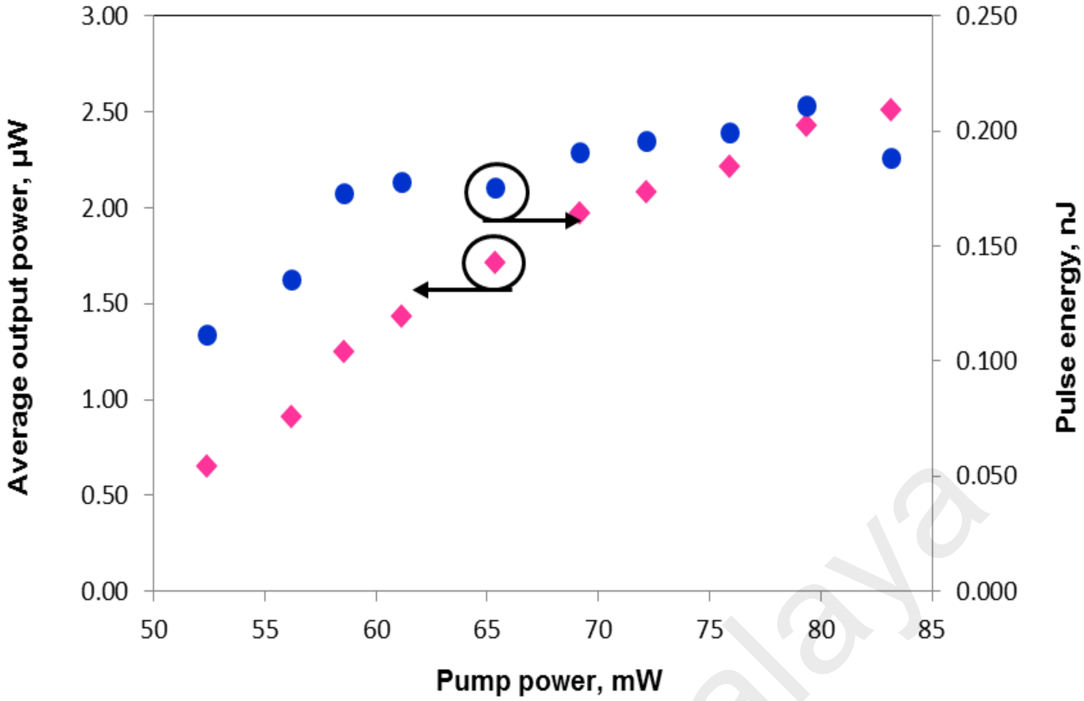

Figure 4.21: The variation of the average output power and pulse energy as the pump power increased from 52.4 mW to 83.2 mW

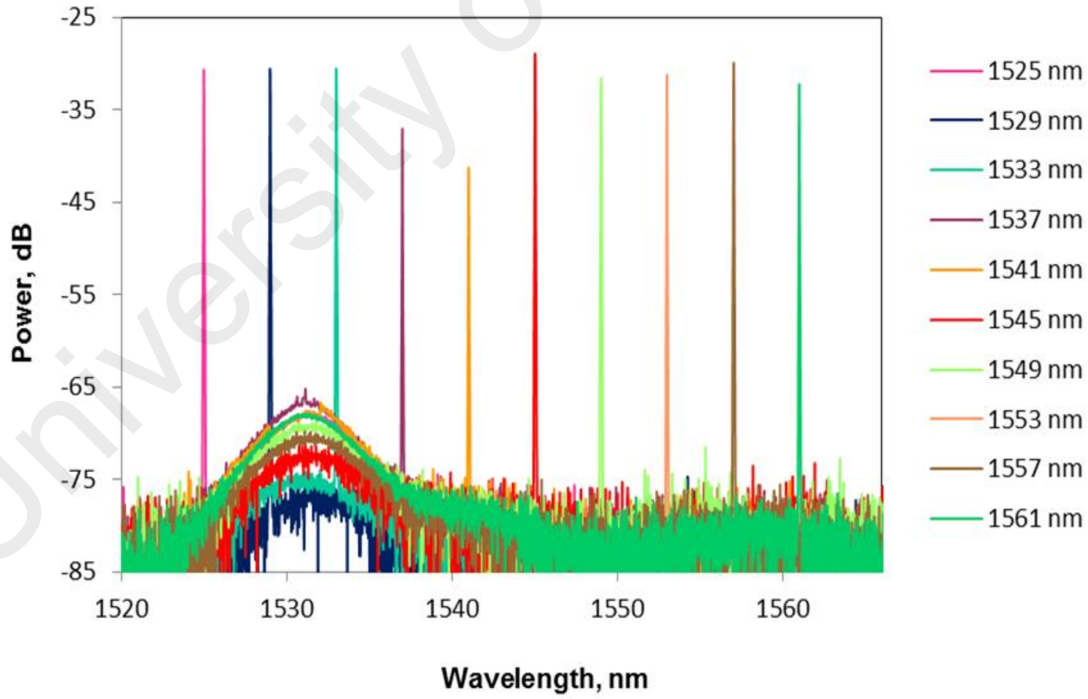

Figure 4.22: Spectra of wavelength-tunable of ultra-narrow linewidth Q-switched operation

To further investigate on the variation of the Q-switched operation during the wavelength-tuning process, the output power, repetition rate and pulse width as functions of the operation wavelength were measured, as shown in Figure 4.23 and 4.24. When the Q-switched wavelength is tuned towards either a longer or a shorter wavelength, the output powers changes to similar to what have been observed in (D. D. Wu et al., 2014) study. The variation of the average output power at different wavelengths could be attributed to the dependences of the EDF's gain spectrum and the cavity loss. From Figure 4.23, the changing pattern of the Q-switched repetition rates with the operation wavelengths is similar to that of the average output power. This can be easily explained as follows. With the larger output power, the intracavity laser is stronger, and the optical transition bleaching of SWCNT SA is faster under a faster population inversion or depletion, leading to faster repetition rates. The fastest and slowest repetition rates achieved is 37.97 kHz at wavelength 1545 nm and 14.84 kHz at wavelength 1541 nm, respectively.

On the other hand, the behavior of the pulse width is the opposite of the repetition rate as shown in Figure 4.24. The widest and most narrow pulse width attained is 5.48 μs and 1.16 μs respectively. The pulse energy at different wavelength operation can be calculated by dividing the average output power with the repetition rate and the value obtained was plotted as in Figure 4.24. The pulse energy varies across the range of wavelength tuning from 1525 nm to 1561 nm. The lowest pulse energy obtained is 0.105 nJ at wavelength 1521 nm and the highest pulse energy attained is 0.181 nJ at wavelength 1545 nm.

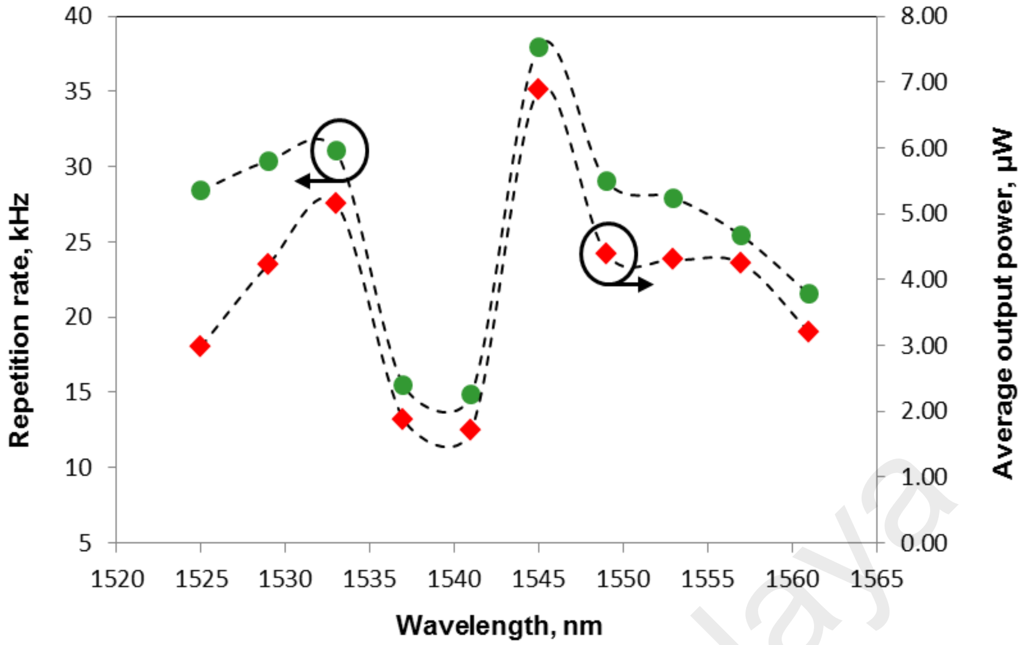

Figure 4.23: Variation of repetition rate and average output power at varied wavelength

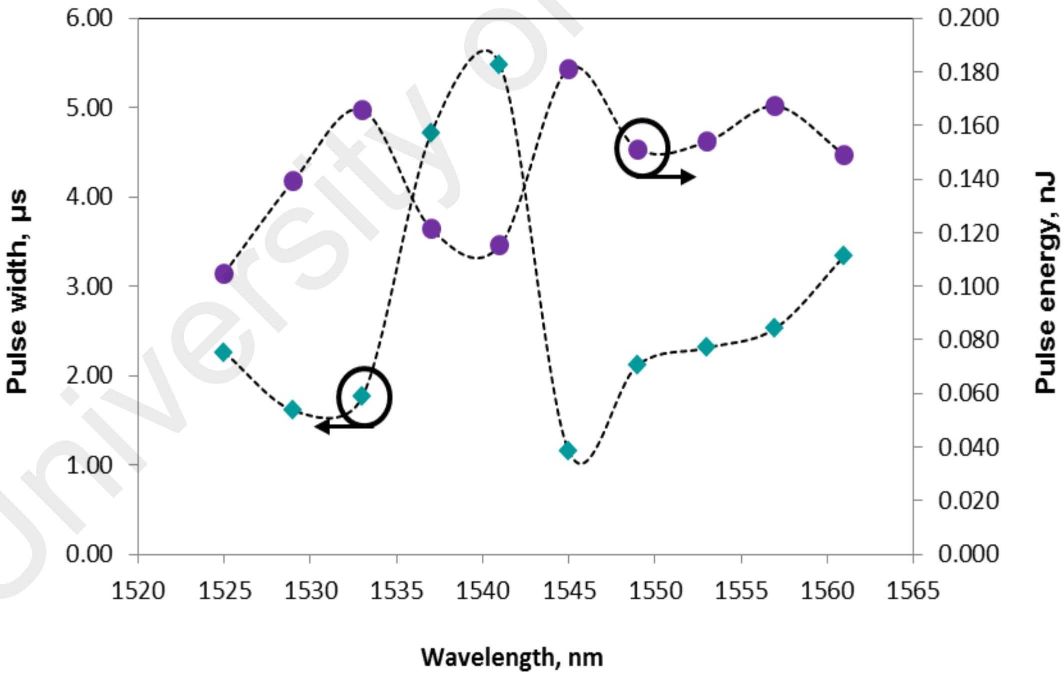

Figure 4.24: Variation of pulse width and pulse energy at varied wavelength

Figure 4.25 (a) and (b) shows the pulse train of the ultra-narrow linewidth of Q-switched pulse retrieved at wavelength operation 1545 and 1541 nm from the oscilloscope. From the figure, the pulse trains are stable and very small fluctuations are observed. Pulse train for wavelength operation of 1545 nm has a pulse interval of 26.42 μs resulting to the repetition rate of37.84 kHz and pulse interval for wavelength operation wavelength of 1541 nm has pulse interval of 67.39 μs, which give the repetition rate of 14.84 kHz

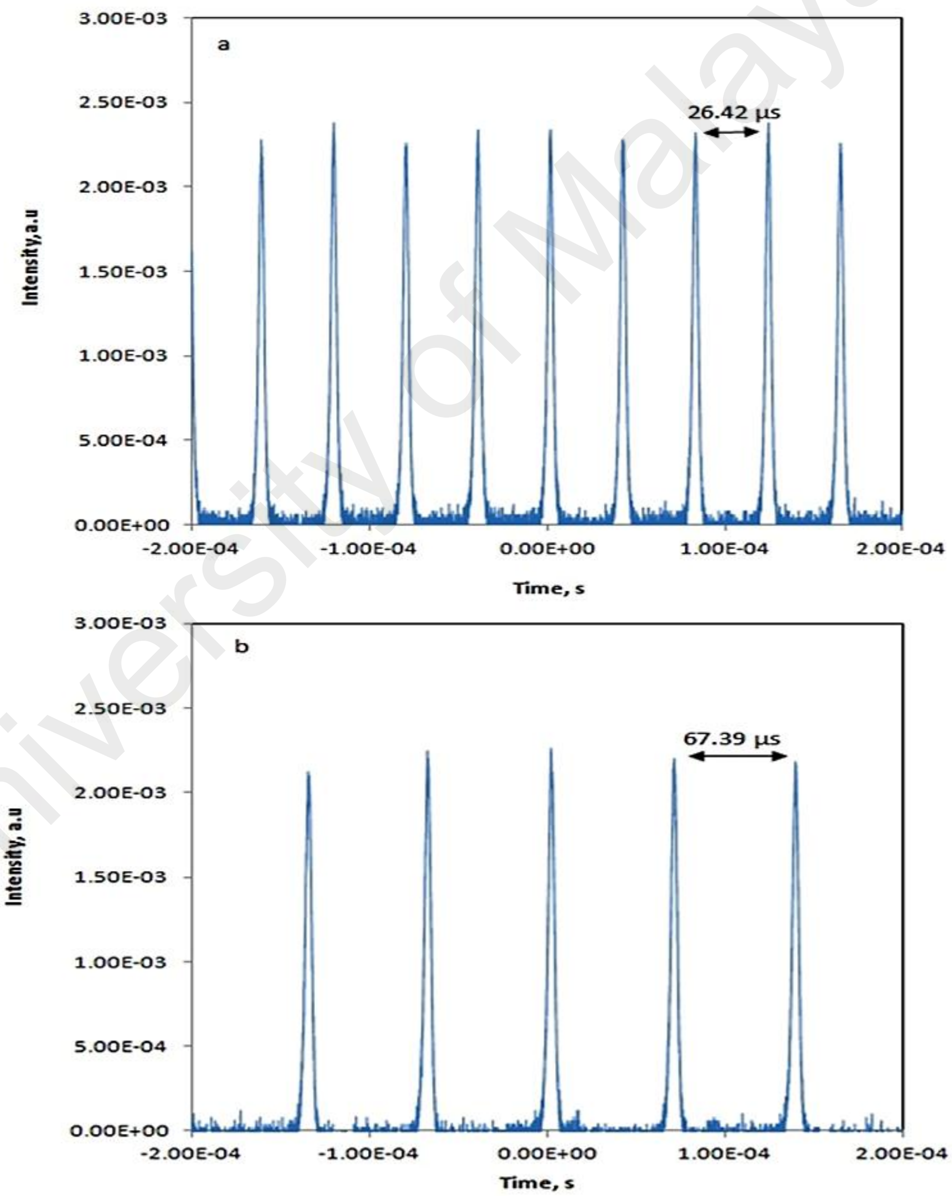

Figure 4.25: Pulse train of the ultra-narrow linewidth of Q-switched pulse retrieved at wavelength operation 1545 and (b) 1541 nm from the oscilloscope

CHAPTER 5: CONCLUSION AND RECOMMENDATION

5.1 Conclusion

The first objective of this work is achieved as the bandwidth, pulse width and wavelength tunability in passively pulsed fiber laser were successfully demonstrated. This work consists of four proposed configurations where the pulse laser is generated by passive approach using SWCNT as saturable absorber. In the first experiment, a tunable pulse width in passively mode-locked fiber laser has been realized by varying the length of polarized maintaining fiber (PMF). Bandwidth of mode-locked spectrum is varied and indirectly tunes the pulse width from 0.52 ps to 1.65 ps. The next experiment is on tunable dual-wavelengths in passively Q-switched fiber laser. A stable dual-wavelength has been demonstrated by using arrayed waveguide grating (AWG) and the wavelength spacing between the two wavelengths is switchable from 1.6 nm to 4.0 nm. Next, the third experiment is on tunable pulsed width in passively Q-switched fiber laser. Bandwidth spectrum of the Q-switched laser is tuned by using an ultra-narrow tunable bandpass filter (UNTBF). As the spectral bandwidth is varied the pulse width is also tuned from 2.6 μs to 5.4 μs. The last experiment is on tunable ultra-narrow linewidth in passively Q-switched fiber laser. The wavelength spectrum can be tuned from 1525 nm to 1561 nm which is about 37 nm in range by using UNTBF.

Then, the second objective of this research is to investigate the performance of the systems proposed have been studied and discussed thoroughly in previous chapter. Hence, both objectives of the research are successfully achieved. In the end of research, it can be concluded that one of most important motivations behind the research of passively pulse fiber laser is compactness as the high cost and the tunability constraint can be overcome. Nevertheless, the flexibility is still restricted compared to actively pulsed fiber laser

5.2 Recommendation

The door to upgrade the flexibility in passively pulsed laser is always open as long as the study on tunability of passively pulsed fiber is continued. In this report, there are parts that could be improved so that the tunability performance of the pulsed laser could be enhanced.

The limitation in range wavelength tunability can be overcome by using other types of saturable absorber such as graphene. Graphene offers the advantages of wavelength independent saturable absorbing properties which are extremely suitable for wide-band tunable laser operation (Cao et al., 2012). It can also lower the threshold value of pulse operation as graphene has larger modulation depth and the damage threshold is much higher. Thus, higher pump power can be applied to the system as it has lower destruction possibility (Ismail et al., 2013). Besides, in the future, the method of tuning can be changed by using different filter with lower loss and different cavity design.

REFERENCES

Ahmad, H., Muhammad, F. D., Zulkifli, M. Z., & Harun, S. W. (2013). Graphene-Based Mode-Locked Spectrum-Tunable Fiber Laser Using Mach-Zehnder Filter. Ieee Photonics Journal, 5(5). doi: Artn 1501709

Doi 10.1109/Jphot.2013.2281609

Ahmad, H., Zulkifli, M., Muhammad, F., Zulkifli, A., & Harun, S. (2013). Tunable graphene-based Q-switched erbium-doped fiber laser using fiber Bragg grating. Journal of Modern Optics, 60(3), 202-212.

Becker, P. M., Olsson, A. A., & Simpson, J. R. (1999). Erbium-doped fiber amplifiers: fundamentals and technology: Academic press.

Bergh, R. A., Culshaw, B., Cutler, C., Lefevre, H. C., & Shaw, H. J. (1982). Source statistics and the Kerr effect in fiber-optic gyroscopes. Optics Letters, 7(11), 563-565.

Boll, R., Anielski, D., Bostedt, C., Bozek, J. D., Christensen, L., Coffee, R., . . . Rolles, D. (2013). Femtosecond photoelectron diffraction on laser-aligned molecules: Towards time-resolved imaging of molecular structure. Phys. Rev. A Physical Review A, 88(6). doi:10.1103/physreva.88.061402

Brabec, T., Spielmann, C., Curley, P., & Krausz, F. (1992). Kerr lens mode locking. Optics Letters, 17(18), 1292-1294.

Caamaño-Tubío, R. I., Pérez, J., Ferreiro, S., and Aldegunde, M. (2007). Peripheral serotonin dynamics in the rainbow trout (Oncorhynchus mykiss). Comparative Biochemistry and Physiology Part C: Toxicology & Pharmacology, 145(2): 245-255

Cakir, Y., and Strauch, S. M. (2005). Tricaine (MS-222) is a safe anesthetic compound compared to benzocaine and pentobaritol to induce anesthesia in leopard frogs (Rana pipiens). Pharmacological Reports, 57: 467-474.

Cameron, A. A., Plenderleith, M. B. and Snow, P. J. (1990). Organization of the spinal cord in four species of elasmobranch fishes: cytoarchitecture and distribution of serotonin and selected neuropeptides. The Journal of Comparative Neurology, 297: 201-218

Cao, W., Wang, H., Luo, A., Luo, Z., & Xu, W. (2012). Graphene-based, 50 nm wide-band tunable passively Q-switched fiber laser. Laser Physics Letters, 9(1), 54.

Cowan, B. (2006). Optical Damage Threshold of Silicon for Ultrafast Infrared Pulses. AIP Conference Proceedings. doi:10.1063/1.2409223

Crombie, A. C. (1990). Expectation, modelling and assent in the history of optics: Part I. Alhazen and the medieval tradition. Studies in History and Philosophy of Science Part A, 21(4), 605-632.

Dutton, H. J. (1998). Understanding optical communications: Prentice Hall PTR.

Fan, Y. X., Lu, F. Y., Hu, S. L., Lu, K. C., Wang, H. J., Zhang, G. Y., & Dong, X. Y. (2003). Narrow-linewidth widely tunable hybrid Q-switched double-clad fiber laser. Optics Letters, 28(7), 537-539. doi: Doi 10.1364/Ol.28.000537

Feng, Z.-Z., Chen, Y.-N., Hsu, J.-M., Lee, C.-L., & Chen, N.-K. (2010). All-fiber Q-switched pulsewidth tunable erbium fiber laser using abrupt-tapered Mach-Zehnder filter. OECC 2010 Technical Digest, 320-321.

Fermann, M. E., Haberl, F., Hofer, M., & Hochreiter, H. (1990). Nonlinear amplifying loop mirror. Optics Letters, 15(13), 752-754.

Frazão, O., Baptista, J. M., & Santos, J. L. (2007). Recent advances in high-birefringence fiber loop mirror sensors. Sensors, 7(11), 2970-2983.

Galili, I., & Hazan, A. (2001). The effect of a history-based course in optics on students' views about science. Science & Education, 10(1-2), 7-32.

Haberl, F., Ober, M., Hofer, M., Fermann, M., Wintner, E., & Schmidt, A. (1991). Low-noise operation modes of a passively mode-locked fiber laser. Photonics Technology Letters, IEEE, 3(12), 1071-1073.

Harun, S. W., Ismail, M. A., Ahmad, F., Ismail, M. F., Nor, R. M., Zulkepely, N. R., & Ahmad, H. (2012). A Q-Switched Erbium-Doped Fiber Laser with a Carbon Nanotube Based Saturable Absorber. Chinese Physics Letters Chinese Phys. Lett., 29(11), 114202. doi:10.1088/0256-307x/29/11/114202

Hecht, J. (1992). Laser pioneers: Academic Press.

Hönninger, C., Paschotta, R., Morier-Genoud, F., Moser, M., & Keller, U. (1999). Q-switching stability limits of continuous-wave passive mode locking. JOSA B, 16(1), 46-56.

Huang, J. Y., Liang, H. C., Su, K. W., Lai, H. C., Chen, Y., & Huang, K. F. (2007). InGaAs quantum-well saturable absorbers for a diode-pumped passively Q-switched Nd:YAG laser at 1123 nm. Appl. Opt. Applied Optics, 46(2), 239. doi:10.1364/ao.46.000239

Ismail, M., Ahmad, F., Harun, S., Arof, H., & Ahmad, H. (2013). A Q-switched erbium-doped fiber laser with a graphene saturable absorber. Laser Physics Letters, 10(2), 025102.

Ismail, M. A., Harun, S. W., Ahmad, H., & Paul, M. C. (2016). Passive Q-switched and Mode-locked Fiber Lasers Using Carbon-based Saturable Absorbers. Fiber Laser. doi:10.5772/61703

Kao, C. K. (1977). Multiple access fiber optical bus communication system: Google Patents.

Kashiwagi, K., & Yamashita, S. (2010). Optical Deposition of Carbon Nanotubes for Fiber-based Device Fabrication: INTECH Open Access Publisher.

Katz, O., & Sintov, Y. (2008). Strictly all-fiber picosecond ytterbium fiber laser utilizing chirped-fiber-Bragg-gratings for dispersion control. Optics Communications, 281(10), 2874-2878. doi: DOI 10.1016/j.optcom.2008.01.048

Lamb, K., Spence, D., Hong, J., Yelland, C., & Sibbett, W. (1994). All-solid-state self-mode-locked Ti: sapphire laser. Optics Letters, 19(22), 1864-1866.

Lee, K., Fok, M., Wan, S., & Shu, C. (2004). Optically controlled Sagnac loop comb filter. Optics Express, 12(25), 6335-6340.

Luo, Z. Q., Zhou, M., Weng, J., Huang, G. M., Xu, H. Y., Ye, C. C., & Cai, Z. P. (2010). Graphene-based passively Q-switched dual-wavelength erbium-doped fiber laser. Optics Letters, 35(21), 3709-3711.

Maiman, T. H. (1960). Stimulated optical radiation in ruby.

Marcos, S., Barbero, S., Llorente, L., & Merayo-Lloves, J. (2001). Optical response to LASIK surgery for myopia from total and corneal aberration measurements. Investigative Ophthalmology and Visual Science, 42(13), 3349-3356.

McCumber, D. (1964). Einstein relations connecting broadband emission and absorption spectra. Physical Review, 136(4A), A954.

Moon, D. S., Kim, B. H., Lin, A., Sun, G., Han, Y.-G., Han, W.-T., & Chung, Y. (2007). The temperature sensitivity of Sagnac loop interferometer based on polarization maintaining side-hole fiber. Optics Express, 15(13), 7962-7967.

Mou, C., Arif, R., Rozhin, A., & Turitsyn, S. (2012). Passively harmonic mode locked erbium doped fiber soliton laser with carbon nanotubes based saturable absorber. Optical Materials Express, 2(6), 884-890.

Nelson, L., Fleischer, S., Lenz, G., & Ippen, E. (1996). Efficient frequency doubling of a femtosecond fiber laser. Optics Letters, 21(21), 1759-1761.

Oehler, A. E. (2009). Multiwave-mode-locked solid-state lasers with up to 100 GHz, applied in a novel broadband telecom source. Diss., Eidgenössische Technische Hochschule ETH Zürich, Nr. 18794, 2009.

Paschotta, D. R. (n.d.). Saturable Absorbers. Retrieved September 04, 2016, from https://www.rp-photonics.com/saturable_absorbers.html

Paschotta, R. (2008). Field guide to laser pulse generation (Vol. 14): SPIE Press Bellington.

Rawicz, A. H. (2008). Theodore Harold Maiman and the invention of laser. Paper presented at the Photonics, Devices, and Systems IV.

Richardson, D., Offerhaus, H., Nilsson, J., & Grudinin, A. (1999). New fibers portend a bright future for high-power lasers. Laser focus world, 35(6), 92-94.

Saraceno, C., Schriber, C., Emaury, F., Heckl, O., Baer, C., Hoffmann, M., . . . Keller, U. (2013). Cutting-Edge High-Power Ultrafast Thin Disk Oscillators. Applied Sciences, 3(2), 355-395. doi:10.3390/app3020355

Schibli, T., Thoen, E., Kärtner, F., & Ippen, E. (2000). Suppression of Q-switched mode locking and break-up into multiple pulses by inverse saturable absorption. Applied Physics B, 70(1), S41-S49.

Siegman, A. E. (1986). Lasers/Anthony E. Siegman: University Science Books, Mill Valley, Calif.

Snitzer, E. (1961). Proposed fiber cavities for optical masers. Journal of Applied Physics, 32(1), 36-39.

Stankov, K. (1988). A mirror with an intensity-dependent reflection coefficient. Applied Physics B, 45(3), 191-195.

Steinmeyer, G., Sutter, D., Gallmann, L., Matuschek, N., & Keller, U. (1999). Frontiers in ultrashort pulse generation: pushing the limits in linear and nonlinear optics. Science, 286(5444), 1507-1512.

Stone, J., & Burrus, C. A. (1973). Neodymium-doped silica lasers in end-pumped fiber geometry. Applied Physics Letters, 23(7), 388-389.

Sun, G., Moon, D. S., Lin, A., Han, W.-T., & Chung, Y. (2008). Tunable multiwavelength fiber laser using a comb filter based on erbium-ytterbium co-doped polarization maintaining fiber loop mirror. Optics Express, 16(6), 3652-3658.

Villanueva, G. E., Ferri, M., & Perez-Millan, P. (2012). Active and passive mode-locked fiber lasers for high-speed high-resolution photonic analog-to-digital conversion. Quantum Electronics, IEEE Journal of, 48(11), 1443-1452.

Villanueva Ibañez, G. E. (2012). Continuous wave and pulsed erbium-doped fiber lasers for microwave photonics applications.

Welford D. (2003). Passively Q-switched lasers. Circuits and Devices Magazine, IEEE, 19(4), 31-6

Woodward, R. I., Kelleher, E. J., Howe, R. C., Hu, G., Torrisi, F., Hasan, T., . . . Taylor, J. R. (2014). Tunable Q-switched fiber laser based on saturable edge-state absorption in few-layer molybdenum disulfide (MoS_2). Opt. Express Optics Express, 22(25), 31113. doi:10.1364/oe.22.031113

Wu, C., & Dutta, N. K. (2000). High-repetition-rate optical pulse generation using a rational harmonic mode-locked fiber laser. Quantum Electronics, IEEE Journal of, 36(2), 145-150.

Wu, D. D., Xiong, F. F., Zhang, C. K., Chen, S. S., Xu, H. Y., Cai, Z. P., . . . Luo, Z. Q. (2014). Large-energy, wavelength-tunable, all-fiber passively Q-switched Er:Yb-codoped double-clad fiber laser with mono-layer chemical vapor deposition graphene. Applied Optics, 53(19), 4089-4093. doi: Doi 10.1364/Ao.53.004089

Xie, G. Q., Tang, D. Y., Luo, H., Zhang, H. J., Yu, H. H., Wang, J. Y., . . . Qian, L. J. (2008). Dual-wavelength synchronously mode-locked Nd : CNGG laser. Optics Letters, 33(16), 1872-1874. doi: Doi 10.1364/Ol.33.001872

Yamashita, S., & Asano, M. (2006). Wide and fast wavelength-tunable mode-locked fiber laser based on dispersion tuning. Optics Express, 14(20), 9299-9306.

Zhang, M., Kelleher, E. J. R., Torrisi, F., Sun, Z., Hasan, T., Popa, D., . . . Taylor, J. R. (2012). Tm-doped fiber laser mode-locked by graphene-polymer composite. Optics Express, 20(22), 25077-25084. doi: Doi 10.1364/Oe.20.025077

Zhu, T., & Huang, S. (2014). Ultra-narrow linewidth fiber laser with self-injection feedback based on Rayleigh backscattering. Paper presented at the CLEO: Science and Innovations.

LIST OF PUBLICATIONS AND PAPERS PRESENTED

1. Ahmad, H., Hamdan, K. Z., Muhammad, F. D., Harun, S. W., & Zulkifli, M. Z. (2015). Switchable dual-wavelength CNT-based Q-switched using arrayed waveguide gratings (AWG). Applied Physics B, 118(2), 269-274.
2. Hamdan, K. Z., 1. Ahmad, H., Zulkifli, M. Z. Controllable pulse width via different lengths of pmf in a sagnac loop passively mode-locked fiber laser. 10th International Symposium on Modern Optics and Its Applications 2015, ISMOA'15.